



저작자표시-변경금지 2.0 대한민국

이용자는 아래의 조건을 따르는 경우에 한하여 자유롭게

- 이 저작물을 복제, 배포, 전송, 전시, 공연 및 방송할 수 있습니다.
- 이 저작물을 영리 목적으로 이용할 수 있습니다.

다음과 같은 조건을 따라야 합니다:



저작자표시. 귀하는 원저작자를 표시하여야 합니다.



변경금지. 귀하는 이 저작물을 개작, 변형 또는 가공할 수 없습니다.

- 귀하는, 이 저작물의 재이용이나 배포의 경우, 이 저작물에 적용된 이용허락조건을 명확하게 나타내어야 합니다.
- 저작권자로부터 별도의 허가를 받으면 이러한 조건들은 적용되지 않습니다.

저작권법에 따른 이용자의 권리는 위의 내용에 의하여 영향을 받지 않습니다.

이것은 [이용허락규약\(Legal Code\)](#)을 이해하기 쉽게 요약한 것입니다.

[Disclaimer](#) 

약학박사학위논문

Evaluation of herb-drug interactions of
xanthophylls and fermented Ginseng extract
focused on inhibitory effects of human hepatic
cytochrome P450s and UDP-glucuronyltransferases

사람 간효소인 cytochrome P450와
UDP-glucuronyltransferases에 대한
억제 효과에 초점을 맞춘 xanthophyll과 발효 인삼
추출물의 허브-약물 상호작용의 평가연구

2014년 2월

서울대학교 대학원

약학과 예방·임상약학 전공

YUFEN ZHENG 정옥분

약학박사학위논문

Evaluation of herb-drug interactions of
xanthophylls and fermented Ginseng extract
focused on inhibitory effects of human hepatic
cytochrome P450s and UDP-glucuronyltransferases

사람 간효소인 cytochrome P450와
UDP-glucuronyltransferase에 대한
억제 효과에 초점을 맞춘 xanthophyll과 발효 인삼
추출물의 허브-약물 상호작용의 평가연구

2014년 2월

서울대학교 대학원

약학과 예방·임상약학 전공

YUFEN ZHENG 정옥분

Evaluation of herb-drug interactions of
xanthophylls and fermented Ginseng extract
focused on inhibitory effects of human hepatic
cytochrome P450s and UDP-glucuronyltransferases

지도교수 신 완 균

이 논문을 약학박사학위논문으로 제출함

2013년 11월

서울대학교 대학원

약학과 예방·임상약학전공

YUFEN ZHENG 정옥분

YUFEN ZHENG 정옥분의 박사학위논문을 인준함

2013년 12월

위 원 장 오 정 미 (인)

부 위 원 장 김 은 경 (인)

위 원 이 명 결 (인)

위 원 이 병 구 (인)

위 원 신 완 균 (인)

TABLE OF CONTENTS

ABSTRACT

LIST OF TABLES

LIST OF FIGURES

A. INTRODUCTION.....	1
B. MATERIALS & METHODS.....	8
C. RESULTS.....	22
D. DISCUSSION & CONCLUSION.....	41
E. REFERENCES.....	47
F. ABSTRACT IN KOREAN.....	57
G. CURRICULUM VITAE.....	61

ABSTRACT

Evaluation of herb–drug interactions of xanthophylls and fermented Ginseng extract focused on inhibitory effects of human hepatic cytochrome P450s and UDP–glucuronosyltransferases

Herb–drug interactions have received more attention recently because of the wide popularity of herbal supplements or dietary supplements. Astaxanthin, β -cryptoxanthin, canthaxanthin, lutein, and zeaxanthin, the major xanthophylls, are widely used and studied because of their activities as antioxidants, their roles in preventing cancer or age-related macular degeneration. BST204, a fermented ginseng extract, contains of high concentrations of Rh2 (over 5.0%) and Rg3 (over 10.0%), whereas crude ginseng extract contains non-detectable Rh2 and only low concentrations of Rg3. It was transformed from the crude ginseng with ginsenoside- β -glucosidase and acid hydrolysis to enrich both 20(R) and 20(S) ginsenoside Rg3 and 20(R) and 20(S) ginsenoside Rh2. Recent studies it showed anti-tumor effects. The object was to investigate the herb–drug interactions of five xanthophylls and BST204 on inhibition of human hepatic cytochrome P450s (CYP1A2, CYP2A6, CYP2B6, CYP2C8, CYP2C9, CYP2C19, CYP2D6, CYP2E1 and CYP3A4/5) and UDP–glucuronosyltransferases (UGT1A1, UGT1A4, UGT1A6, UGT1A9, UGT2B7) in human liver microsomes. We also first explore the stereo selective effects of ginsenoside Rg3 and Rh2 enantiomers (R–Rg3, S–Rg3, R–Rh2 and S–Rh2)

on the inhibitory effects of human hepatic cytochrome P450s and UDP-glucuronosyltransferases.

According to USFDA guidelines, phenacetin (50 μM), coumarin (5 μM), bupropion (50 μM), rosiglitazone (1 μM), tolbutamide (100 μM), S-mephenytoin (100 μM), dextrophan (5 μM), chlorzoxazone (50 μM) and midazolam (5 μM) were chosen as substrates of CYP1A2, CYP2A6, CYP2B6, CYP2C8, CYP2C9, CYP2C19, CYP2D6, CYP2E1 and CYP3A, respectively. Cocktails, test compounds and NADPH re-generating system were incubated 15min after 5 pre-incubation with human liver microsomes (HLMs) in vitro for competitive screening. Time-dependent inhibition (TDI) experiments were also executed. The xanthophylls, HLMs with/without NADPH were incubated at 37°C for 30 min and then were partly shifted to substrates solutions for continued 15 min incubations. On the other hand, we chose β -estradiol (10 μM), trifluoperazine (40 μM), serotonin (4000 μM), propofol (100 μM), and zidovudine (100 μM) as substrates of UGT1A1, UGT1A4, UGT1A6, UGT1A9, and UGT2B7, respectively. Test compounds, human liver microsomes (HLMs) (0.25 mg/ml), 100 mM Tris-HCl buffer (pH 7.5), MgCl_2 (5 mM), substrate, and alamethicin (25 $\mu\text{g/mL}$) were pre-incubated on ice to allow alamethicin pore formation in vitro for 30 min. Incubations were commenced with the addition of UDPGA (5 mM) to a final incubation volume of 0.1 ml and incubated at 37°C for 30 min or 60 min.

The results showed that xanthophylls and fermented Ginseng extract play ignorable effects on the reversible and irreversible inhibitions of 9 CYPs. But, β -cryptoxanthin, canthaxanthin and zeaxanthin showed

inhibitory effects on UGT1A1 with IC_{50} 23.68, 36.74 and 42.57 μ M, respectively. β -cryptoxanthin and lutein also played inhibitory effect on UGT1A4. BST204 inhibited UGT1A1, 1A9, 2B7 with IC_{50} values 13.80, 24.59 and 30.83 μ g/mL, respectively. S-Rg3, not R-Rg3, showed inhibitory interaction toward UGT1A9 and 2B7. Kinetic constants (K_i) of BST204 on UGT1A1, 1A9, 2B7 enzymes were 27.38, 17.53, 32.51 μ g/mL, respectively. The K_i of S-Rg3 inhibited UGT1A9 and 2B7 were 8.33 and 24.89 μ M, respectively.

Based on the IC_{50} values of these five xanthophylls and fermented Ginseng extract (BST204) on CYPs were markedly greater than the C_{max} values, it is unlikely that these five xanthophylls, and BST204, from the diet or nutritional supplement alter the pharmacokinetics of drugs metabolized by CYPs. In addition, the inhibitory effects of xanthophylls on UGTs were ignored due to the much higher IC_{50} or K_i . However, further study about BST204 on the inhibition of UGT1A1, UGT1A9, UGT2B7 are still needed. These findings provide some useful information for the safe and effective use of these herbs in clinical practice.

Key Words: herb-drug interaction, xanthophylls, BST204,
Ginseng extract, LC-MS/MS

Student Number: 2011-30824

LIST OF TABLES

Table 1. P450-selective and UGTs substrates, their concentrations, metabolites and each positive control.

Table 2. MRM transition and mass spectrometry parameters for the analysis in the LC-MS/MS method.

Table 3. IC₅₀ of astaxanthin, β -cryptoxanthin, canthaxanthin, lutein, zeaxanthin and fermented Ginseng extract BST204, ginsenoside Rg3 R-form, Rg3 S-form, Rh2 R-form and Rh2 S-form (R-Rg3, S-Rg3, R-Rh2, S-Rh2) on 9 CYP isozyme activities in pooled human liver microsomes.

Table 4. IC₅₀ of astaxanthin, β -cryptoxanthin, canthaxanthin, lutein, zeaxanthin and fermented Ginseng extract BST204, ginsenoside Rg3 R-form, Rg3 S-form, Rh2 R-form and Rh2 S-form (R-Rg3, S-Rg3, R-Rh2, S-Rh2) on 5 UGT isozyme activities in pooled human liver microsomes.

Table 5. Pharmacokinetic parameters of ginsenoside Rg3 S-form and Rh2 S-form (S-Rg3, S-Rh2) after single oral administration of BST204 extract at doses of 100 mg and 400 mg to healthy volunteer.

LIST OF FIGURES

Figure 1. Chemical structures of astaxanthin (A), β -cryptoxanthin (B), canthaxanthin (C), lutein (D), and zeaxanthin (E).

Figure 2. (A)~(D). Chemical structures of ginsenoside Rg3 R-form, ginsenoside Rg3 S-form, ginsenoside Rh2 R-form and ginsenoside Rh2 S-form.

Figure 3. (A)~(E). Inhibition of CYP1A2, CYP2A6, CYP2B6, CYP2C8, CYP2C9, CYP2C19, CYP2D6, CYP2E1, and CYP3A4/5 by astraxanthin (A), β -cryptoxanthin (B), canthaxanthin (C), lutein (D), and zeaxanthin (E) in human liver microsomes. Each data point represents the mean value of triplicate determinations.

Figure 4. (A)~(E). Inhibitory effects of BST204, Rg3 R-form, Rg3 S-form, Rh2 R-form, and Rh2 S-form on 9 CYP isoforms in pooled human liver microsomes. The activity of each isoform was measured using respective specific probe substrate reaction. Represented by % of control activity.

Figure 5. Representative IC_{50} shift plots for CYP3A4/5 by canthaxanthin with human liver microsomes in the presence (●) and absence (○) of NADPH for 30 min pre-incubation. Each data point represents the mean value of triplicate determinations. Vertical bars

represent standard error of the mean.

Figure 6. Time-dependent inhibitory effects of BST204 using IC_{50} shift assay on nine CYP isozymes. The activity of each isoform was measured using respective specific probe substrate reaction ((●) with NADPH and (○) without NADPH). Represented by % of control activity. All experiments were conducted as duplicate.

Figure 7. Inhibition of UGT1A1, UGT1A4, UGT1A6, UGT1A9 and UGT2B7 by astraxanthin(A), β -cryptoxanthin (B), canthaxanthin (C), lutein (D), and zeaxanthin (E) in human liver microsomes. Each data point represents the mean value of triplicate determinations.

Figure 8. UGTs (UGT1A1, 1A4, 1A6, 1A9, 2B7) inhibitory effects of BST204, ginsenoside Rg3 R-form, Rg3 S-form, Rh2 R-form, and Rh2 S-form. The activity was measured using respective specific probe substrate reaction. Represented by % of control activity. All experiments were conducted as duplicate.

Figure 9. (A) Lineweaver-Burk plot and (B) Dixon plot about the K_i determination of β -cryptoxanthin towards UGT1A1-mediated glucuronidation. All the experiments were carried out in duplicate.

Figure 10. Dixon plot and Lineweaver-Burk plot about the K_i determination of BST204 towards UGT-mediated glucuronidation. (A) BST204 on UGT1A1-mediated estradiol glucuronidation; (B) BST204

on UGT1A9-mediated propofol glucuronidation; (C) BST204 on UGT2B7-mediated zidovudine glucuronidation. All the experiments were carried out in duplicate.

Figure 11. Dixon plot and Lineweaver-Burk plot about the K_i determination of ginsenoside Rg3 S-form towards UGT-mediated glucuronidation. (A) Ginsenoside Rg3 S-form on UGT1A9-mediated estradiol glucuronidation; (B) Ginsenoside Rg3 S-form on UGT2B7-mediated zidovudine glucuronidation. All the experiments were carried out in duplicate.

Figure 12. Mean plasma concentrations of ginsenoside Rg3 S-form (S-Rg3: A; circle) and ginsenoside Rg3 S-form (S-Rh2: B; square) after single oral administration of BST204 extract at doses of 100 mg (closed, n=5) and 400 mg (open, n=5) to human volunteers.

A. INTRODUCTION

Although drug–drug interactions may be identified during drug development and approval, food/supplement–drug interactions should not be overlooked. Natural health products are being increasingly widely used. Apart from an appraisal of product safety and effectiveness, attention should be paid to the potential that these product ingredients may interact with medications (Bailey and Dresser, 2004). Unpredicted drug–drug interactions have led to severe adverse effects or failure to treatments. Many of these interactions involve inhibition or induction of drug–metabolizing cytochrome P450 (CYPs) and UDP–glucuronosyltransferases (UGTs) enzymes. Similarly, dietary supplement or nutrients may be inhibitors of CYP or UGT enzymes and have an effect on the pharmacokinetics of any co–medicated drugs.

The xanthophylls, a major group of carotenoids, primarily include astaxanthin, β -cryptoxanthin, canthaxanthin, lutein, zeaxanthin and so on (Figure 1). They have been widely used and studied as beneficial food components associated with their antioxidant activities (Miller et al., 1996) and the possibility of their use reducing the incidence of chronic diseases (Higuera - Ciapara et al., 2006). Astaxanthin, one of the main pigments in crustacean, salmonid, and other farmed fish feed, has been used for protecting organisms against a wide range of ailments, such as cardiovascular problems, diabetes, chronic inflammatory diseases, different types of cancer, and some diseases of the immunological system due to its outstanding antioxidant activities (Higuera - Ciapara et al., 2006; Hussein et al., 2006; Yuan et al., 2011). β -cryptoxanthin, found in fruits and vegetables such as green grapes,

coriander, parsley, and basil, has been shown to function as an antioxidant in many *in vitro* systems (Lorenzo et al., 2009). Intake of a canthaxanthin-rich diet has been associated with a decreased risk of cancer (Jewell and O'Brien, 1999). Interestingly, canthaxanthin is widely used as a food color additive and is also included in pharmaceutical tablets used for photosensitive disorder treatments and tanning pills (Lyan et al., 2001). Lutein and zeaxanthin are two major carotenoids in the human macula and retina (Bone et al., 1988; Handelman et al., 1988). In the diet, dark green leafy vegetables, corn, and egg yolk contain the highest concentrations of lutein (Sommerburg et al., 1998). Zeaxanthin is found in corn, orange pepper, oranges, and tangerines. Lutein and zeaxanthin are important nutrients for the prevention of age-related macular degeneration (Richer et al., 2004; Zhao and Sweet, 2008; Ma et al., 2012). Unpredicted drug-drug interactions have led to severe adverse effects or failure to treatments. Many of these interactions involve inhibition or induction of drug-metabolizing CYP enzymes (Iwata et al., 2005). There are few reports of about interactions between drug-metabolizing enzymes and these five xanthophylls. Gradelet et al (1996) reported that astaxanthin and canthaxanthin were substantial inducers of phase I enzymes such as CYP1A1, CYP1A2, and the phase II enzyme 4NP UGT in rats. β -cryptoxanthin resulted in a 23% increase in liver glutathione S-transferase activity in rats (Gradelet et al., 1996). In human hepatocytes, astaxanthin appeared to induce CYP2B6 and CYP3A4 (Kistler et al., 2002). However, the inhibitory activities of these xanthophylls on CYPs and UGTs

isozymes in human liver microsomes have been little investigated.

As we know, ginsenosides were the main components of Ginseng, which is the widely used as a key herb in Asian countries associated with the benefit of immune functions, blood pressure, metabolites, cancer, endocrine, cardiovascular, and so on (Attele et al., 1999; Chen et al., 2008). Unlike crude ginseng extract with non-detectable Rh2 and only low concentrations of Rg3, BST204 contains of high concentrations of Rh2 (over 5.0%)

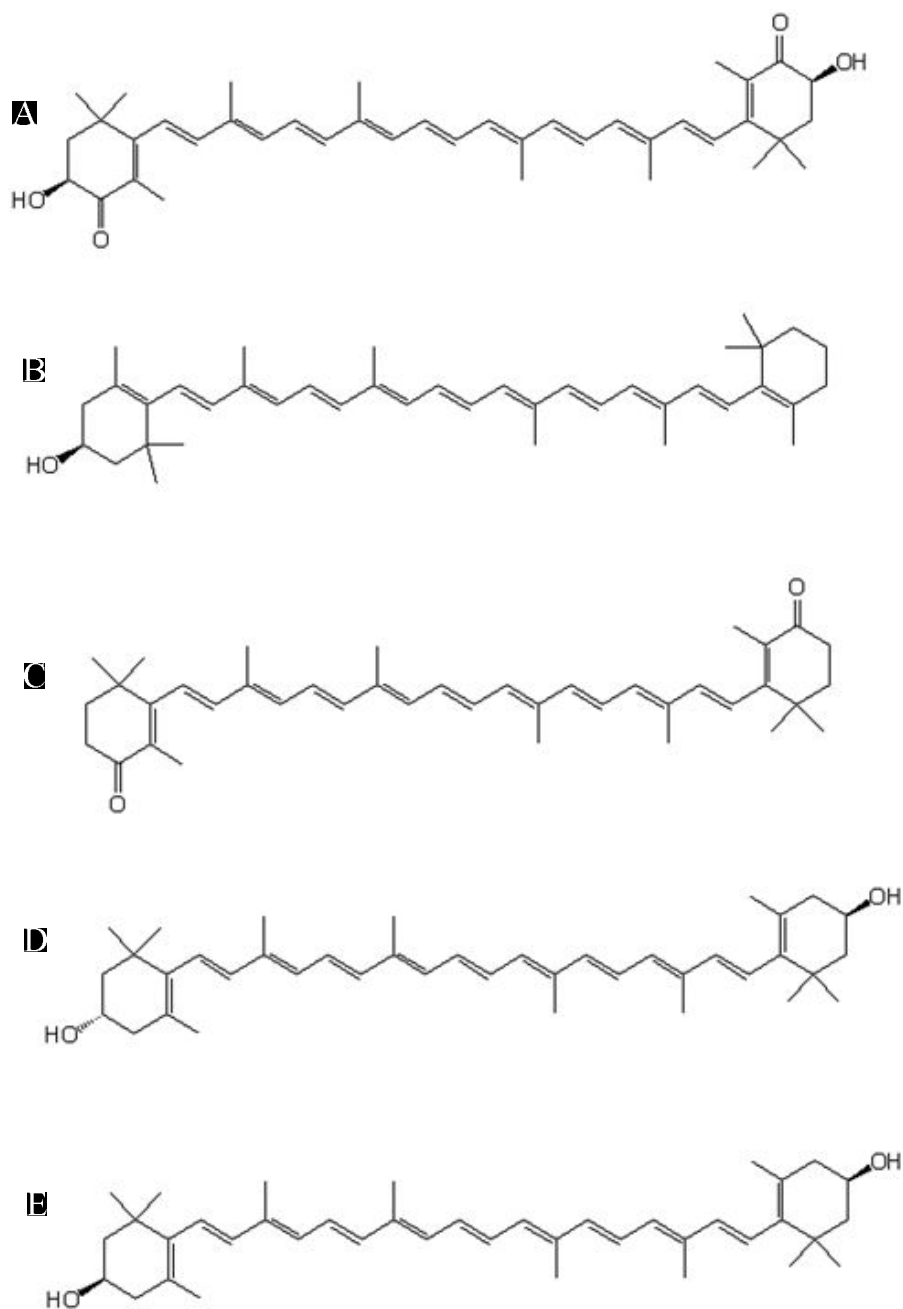


Figure 1. Chemical structures of astaxanthin (A), β -cryptoxanthin (B), canthaxanthin (C), lutein (D), and zeaxanthin (E).

and Rg3 (over 10.0%) that may support better effects to people (Seo et al., 2005a). It was a transformed form of the crude ginseng with ginsenoside- β -glucosidase and acid hydrolysis to enrich both 20(R) and 20(S) ginsenoside Rg3 and 20(R) and 20(S) ginsenoside Rh2 (R-Rg3, S-Rg3, R-Rh2 and S-Rh2, Figure 2), which have been shown anti-tumor effects (Seo et al., 2005b, Yang et al., 2012). Much research has been focused on the stereoselective pharmacological effects of ginsenoside Rg3 and Rh2 epimers. For example, Wei has demonstrated that Rg3 was stereo specific in antioxidant activities as R or S exhibited significantly higher antioxidant effects than S form (Wei et al. 2012a); 20(R)-Rg3 has more potent adjuvant activity than 20(S)-Rg3 related to stereo specific stimulation of the immune response (Wei et al., 2012b); however, 20(S)-ginsenoside Rg3 showed antioxidative, anti-inflammatory, and matrix metalloproteinase inhibitory activities in cultured mammalian cell lines (Shin et al., 2013); Only ginsenoside 20(R)-Rh2 showed selective osteoclastogenesis inhibitory activity without any cytotoxicity (Li et al., 2010); 20(S)-Ginsenoside Rh2 against doxorubicin-induced cardiotoxicity (Wang et al., 2012); Only ginsenoside 20(S)-Rh2 showed proliferation inhibition on androgen-dependent and -independent prostate cancer cells (Liu et al., 2010). These results implied that the stereochemistry of the hydroxyl group at C-20 may play an important role in pharmacological activities. So, it implied us that structural isomerism may also show different impacts during drug metabolism.

The aim of the present study is to investigate the herb-drug

interactions of five xanthophylls and BST204 on inhibition of human hepatic cytochrome P450s and UDP-glucuronosyltransferases in human liver microsomes. We also first explore the stereoselective effects of ginsenoside Rg3 and Rh2 enantiomers (R-Rg3, S-Rg3, R-Rh2 and S-Rh2) on the inhibitory effects of CYPs and UGTs.

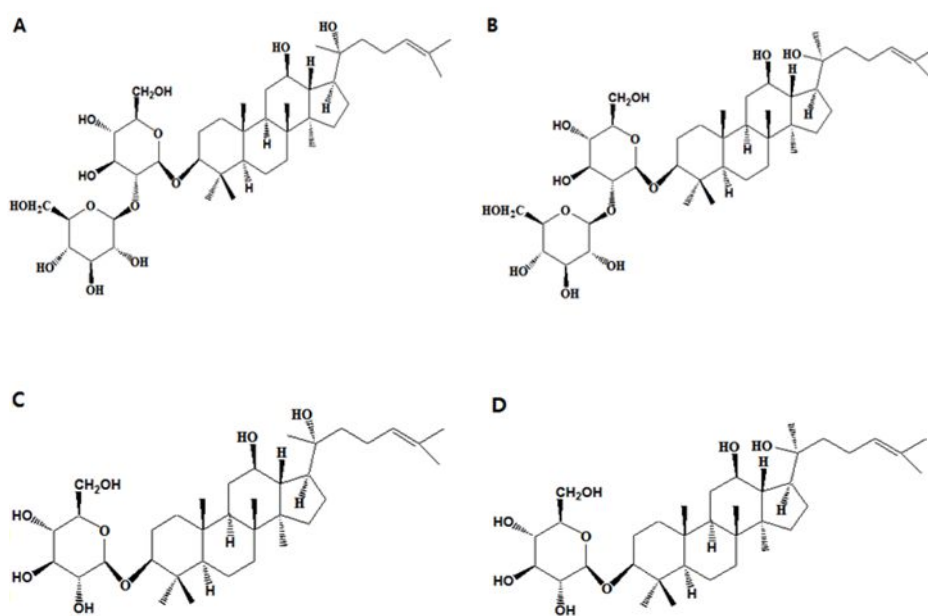


Figure 2. (A)~(D). Chemical structures of ginsenoside Rg3 R-form, ginsenoside Rg3 S-form, ginsenoside Rh2 R-form and ginsenoside Rh2 S-form.

B. MATERIALS & METHODS

Materials

R-Rg3 (purity, 91.2%), S-Rg3 (purity, 93.6%), R-Rh2 (purity, 96.23%) and S-Rh2 (purity, 98.9%) (Fig. 1) and BST204 extract (Lot No. S203; which is contained of Rh2, 6.3% and Rg3, 13.6%), were provided by Green Cross Herb & Pharmaceutical Co., Ltd (Sungnam, Republic of Korea). Dioscin (purity \geq 99%) was obtained from Dr. Kee Dong Yoon, professor of the Catholic University of Korea. Pooled human liver microsomes from a mixed pool of 50 donors were purchased from BD Gentest (Woburn, MA, USA). Astaxanthin, β -cryptoxanthin, lutein, β -nicotinamide adenine dinucleotide phosphate (NADP), glucose-6-phosphate, glucose-6-phosphate dehydrogenase, MgCl₂, acetaminophen, chlorzoxazone, coumarin, dextrorphan, diethyldithiocarbamate, furafylline, ketoconazole, monterukast, paclitaxel, sulfaphenazole, S-mephenytoin, S-benzylirvanol, phenacetin, quinidine, tolbutamide, tranlycypromine, triethylenethiophoramide, uridine 5'-diphosphoglucuronic acid trisodium salt (UDPGA), alamethicin, β -estradiol, trifluoperazine dihydrochloride, 3'-azido-3'-deoxythymidine (zidovudine), chrysin, hecogenin, serotonin hydrochloride, 1-naphthol, niflumic acid, chlorpropamide, theophylline and formic acid were purchased from Sigma-Aldrich (St. Louis, MO, USA). Bupropion, dextromethorphan, 4'-hydroxymephenytoin, 7 hydroxycoumarin, 1'-hydroxychlorzoxazone, 1'-hydroxymidazolam, midazolam, 6 α -hydroxypaclitaxel, propofol, efavirenz, canthaxanthin, and zeaxanthin were purchased from Toronto Research Chemicals (North York, ON, Canada). All solvents were of high-performance

liquid chromatography (HPLC) grade and were obtained from Fisher Scientific Company (Pittsburgh, PA, USA) and other chemicals were of the highest quality available.

Competitive inhibitory effects of xanthophylls and fermented Ginseng extract nine cytochrome P450 enzymes

So-called cocktail assays in which several enzyme activities are determined in parallel by liquid chromatography - tandem mass spectrometry (LC-MS/MS) are particularly useful. The inhibitory potencies of astaxanthin, β -cryptoxanthin, canthaxanthin, lutein, zeaxanthin BST204 and the four ginsenosides R-Rg3, S-Rg3, R-Rh2 and S-Rh2 were determined with nine CYP enzyme cocktail assays as previously described (Kim et al., 2005) with slight modification. In brief, the 90- μ L incubation mixture, including pooled human liver microsomes (final concentration 0.25 mg/mL), 0.1 M phosphate buffer (pH 7.4), each P450-selective substrates cocktail set (A set: phenacetin, coumarin, paclitaxel, S-mephenytoin, dextromethorphan, and midazolam; B set: bupropion, tolbutamide, and chlorzoxazone), and test compounds was pre-incubated for 5 min at 37°C. Test compounds were dissolved in DMSO and diluted in 0.1 M phosphate buffer (pH 7.4), to a final concentration of 0.5% DMSO. Concentrations of P450-selective substrates were used close to their reported Km values (Yuan et al., 2002): 50 mM phenacetin (CYP1A2), 5 mM coumarin (CYP2A6), 10 mM paclitaxel (CYP2C8), 100mM tolbutamide (CYP2C9), 100mM S-mephenytoin (CYP2C19), 5 mM

dextromethorphan (CYP2D6), 50 mM chlorzoxazone (CYP2E1), and 5 mM midazolam (CYP3A4/5). All of P450-selective substrates were dissolved in methanol and serially diluted with methanol to the required concentrations, and the solvent was subsequently evaporated under reduced pressure using an AES2010 SpeedVac (Thermo Electron Co., Waltham, MA). On the other hand, coumarin dissolved in methanol was added directly to the mixed tube (a final concentration of 0.5% methanol) because of its low solubility in 0.1 M phosphate buffer (pH 7.4). P450-selective substrates and their concentrations, metabolites, and positive control were shown in Table 2.

The reaction was started by adding a 10- μ L NADPH-generating system (1.3 mM NADP⁺, 3.3 mM glucose-6-phosphate, 3.3 mM MgCl₂, and 0.4 unit/mL glucose-6-phosphate dehydrogenase). The reaction system (100 μ L, total volume) was incubated for 15 min at 37°C in a shaking water bath. After incubation, reactions were stopped by addition of 50 μ L of ice-cold acetonitrile containing 2 μ M chlorpropamide, as an internal standard, and they were chilled and centrifuged (13,000 rpm, 8 min, 4°C). Mixture of A set and B set (1:1) were diluted 100-fold with acetonitrile and then injected into the LC MS/MS system. All incubations were performed in triplicate, and mean values were used for analysis. Additionally identical parallel incubation samples containing known direct CYP inhibitors were included as positive controls.

Time-dependent inhibition of xanthophylls and fermented Ginseng extract on nine cytochrome P450 enzymes

To assess time-dependent inhibitory potentials of test compounds, single point inactivation experiments were used as previously reported (Obach et al. 2007). In brief, pooled human liver microsomes (1 mg/mL) were incubated with test compounds in the absence and presence of NADPH-generating system for 30 min at 37°C. After incubation, an aliquot (10 μ L) was transferred to another incubation tube (final volume 100 μ L) containing an NADPH-generating system and each P450-selective substrates cocktail set (both A and B sets). The reaction system (100 μ L, total volume) was incubated for 15 min at 37°C in a shaking water bath. Other procedures were similar to those of the reversible inhibition studies.

Inhibitory effects of xanthophylls and fermented Ginseng extract on UGTs

We chose β -estradiol (10 μ M), trifluoperazine (40 μ M), serotonin (4000 μ M), propofol (100 μ M), and zidovudine (100 μ M) as substrates of UGT1A1, UGT1A4, UGT1A6, UGT1A9, and UGT2B7, respectively. Test compounds, human liver microsomes (HLMs) (0.25 mg/mL), 100 mM Tris-HCl buffer (pH 7.5), MgCl₂ (5 mM), substrate, and alamethicin (25 μ g/mL) were pre-incubated on ice to allow alamethicin pore formation in vitro for 30 min. Incubations were commenced with the addition of 10 μ L UDPGA (5 mM) to a final

incubation volume of 0.1 mL and incubated at 37°C for 60min (except 30 min for UGT1A9) at 37°C in a shaking water bath. Final solvent concentrations were 5% (v/v) DMSO. After incubation, the reaction was stopped by adding 50 μ L of ice-cold acetonitrile containing 300 ng/ml chlorpropamide or 300 μ g/mL theophylline as an internal standard. The incubation mixtures were then centrifuged (13,000 g for 15 min at 4°C). Aliquots of the supernatants were injected into a LC-MS/MS system. Known potent inhibitors, chrysin, hecogenin, 1-naphthol, niflumic acid, and efavirenz, were included as positive controls to evaluate the suitability of these experiments and to compare their IC_{50} values to UGT1A1, UGT1A4, UGT1A6, UGT1A9, and UGT2B7, respectively. UGT substrates and their concentrations, metabolites, and positive control were shown in Table 2. All substrates and inhibitors used as positive controls are selected according to several published papers (Fujiwara et al., 2008; Krishnaswamy et al., 2003; Miners J.O., et al., 2011; Uchaipichat et al., 2006; Walsky et al., 2012; Belanger et al., 2009). All incubations were performed in duplicate, and mean values were used for analysis. All P450-selective and UGT substrates, their concentrations, metabolites and each positive control were shown in Table 1.

Table 1. P450-selective and UGTs substrates, their concentrations, metabolites and each positive control.

Enzymes	Substrates	Final Conc.	Metabolites	Positive Control
CYP1A2	Phenacetin	50µM	Acetaminophen	Furafylline
CYP2A6	Coumarin	5µM	Oh-coumarin	Tranlycypromine
CYP2B6	Bupropion	50µM	Oh-bupropion	Triethylenethiophoramide
CYP2C8	Rosiglitazone	1µM	Oh-rosiglitazone	Monterukast
CYP2C9	Tolbutamide	100µM	Oh-tolbutamide	Sulfaphenazole
CYP2C19	<i>S</i> -mephenytoin	100µM	Oh-mephenytoin	S-Benzylirvanol
CYP2D6	Dextromethorphan	5µM	Dextrorphan	Quinidine
CYP2E1	Chlorzoxazone	50µM	Oh-chlorzoxazone	Diethyldithiocarbamate
CYP3A4/5	Midazolam	5µM	Oh-midazolam	Ketoconazole
UGT1A1	β -estradiol	10µM	β -estradiol-3-Glucuronide	Chrysin
UGT1A4	Trifluoperazine	40µM	Trifluoperazine N-Glucuronide	Hecogenine
UGT1A6	Serotonin	4000µM	Serotonin-O-Glucuronide	1-Naphthol
UGT1A9	Propofol	100µM	Propofol-O-Glucuronide	Niflumic acid
UGT2B7	Zidovudine	100µM	AZT-5'-Glucuronide	Efavirenz

K_i determination of β -cryptoxanthin, BST204, S-Rg3 on UGT1A1, 1A9, or 2B7

Based on the IC₅₀ values, the experiments for the determination of K_i values of β -cryptoxanthin on UGT1A1, BST204 on UGT1A1, 1A9 and 2B7, S-Rg3 on UGT1A9 and UGT2B7 were conducted. The experiments for the determination of K_i values of UGT1A1-catalyzed estradiol 3-glucuronidation reaction, UGT1A9-catalyzed propofol glucuronidation and UGT2B7-catalyzed 3'-azido-3'-deoxythymidine glucuronidation were selected as the probe reactions. Chrysin, niflumic acid and efavirenz were included as positive controls. The concentration of substrates was determined near the K_m values: estradiol was 50, 10, and 20 μ M, propofol was 5, 10, 100 μ M, and zidovudine was 25, 100, 200 μ M, respectively. The reaction rates were linear with incubation time and microsomal protein contents under these conditions. Dixon and Lineweaver-Burk plots were adapted to determine the inhibition type, and the second plot of slopes from Lineweaver - Burk plot versus test compound concentrations was utilized to calculate the K_i value. All incubations were performed in duplicate, and mean values were used for analysis.

Pharmacokinetic study of BST204 in health volunteers

Blood from each healthy volunteer was collected at 0, 0.5, 1, 2, 4, 6, 8, 12 and 24 h after oral 100 mg (n=5) and 400 mg (n=5) BST204. 1 mL of human plasma samples were transferred into a glass tube and spiked with 20 μ L IS solution containing dioscin 5 μ g/mL (Bae et al. 2013). The mixture was extracted with 4 mL of ethyl acetate by vortexing for 15 min for extraction. The pharmacokinetic parameters were calculated by a non-compartmental analysis (WinNonlin Professional ver. 5.2, Pharsight, Mountain View, CA, USA) for determining the followings: the total area under the plasma concentration - time curve from time zero to infinity ($AUC_{0-\infty}$) or the last measured time (AUC_t). The peak plasma concentration (C_{max}) and time to reach C_{max} (T_{max}) were taken directly from the experimental data.

LC-MS/MS analysis

Metabolites of nine P450-selective substrates were analyzed using a tandem quadrupole mass spectrometer (QTrap 5500 LC-MS/MS, Applied Biosystems, Foster City, CA) equipped with an electrospray ionization (ESI) interface used to generate positive and negative ion mode. The separation was performed on a reversed-phase column (Luna C₁₈, 50 mm × 2.0 mm i.d.; 3 μm particle size; Phenomenex, Torrance, CA) maintained at 40°C. Mobile phase consisted of acetonitrile (A) and water containing 0.1% formic acid (B) at a flow rate of 0.5 mL/min. The gradient elution program used was as follows: (1) mobile phase A was set to 85% at 0 min, (2) a linear gradient was run to 20% in 2.6 min, and (3) a linear gradient was run to 85% in 3.5 min, and re-equilibrated for 2.5 min. The total run time was 6 min. An Agilent 1260 series high-performance liquid chromatography system (Agilent, Wilmington, DE), was used.

For UGTs substrate analysis, a tandem quadrupole mass spectrometer (QTrap 3200 LC-MS/MS; AB Sciex, Foster City, CA, USA) and HPLC system (Agilent 1260 series, Wilmington, DE, USA) were used and the separation was performed on a reversed-phase column (Poroshell 120 C₁₈, 50 mm × 4.6 mm i.d.; 2.7 μm particle size; Agilent, Wilmington, DE, USA) maintained at 40°C. Single reaction monitoring mode using specific precursor/product ion transition was used for the quantification. The mass transitions of the metabolites of nine P450-selective substrates and 5 UGT substrates and 2 internal standards are listed in Table 1. Peak areas for all the analytes were

automatically integrated using Analyst software (version 1.5.2, Applied Biosystems, Foster City, CA).

For pharmacokinetic study of ginsenosides, we chose API 5500 Q-Trap mass spectrometer (AB Sciex, Foster City, CA) equipped with Agilent 1290 HPLC system (Agilent Technologies, Wilmington, DE) in an electrospray ionization (ESI) mode used to generate negative $[M - H]^-$. The compounds were separated on a reversed-phase column (Acclaim RSLC C₁₈ column 150 × 2.1 mm, 2.2- μ m particle size; Thermo) maintained at 40°C. The MRM transition and mass spectrometry parameters for all the analysis in the LC-MS/MS method were shown in Table 2.

Table 2. MRM transition and mass spectrometry parameters for the analysis in the LC-MS/MS method.

Analytes	MRM (m/z)	Dwell Time (msecs)	DP (volts)	CE (volts)	CXP (volts)	Polarity
Acetaminophen	152.0>110.1	200	46	21	12	Positive
Oh-coumarin	160.8>132.9	150	-90	-28	-11	Negative
Oh-bupropion	256.3>238.1	150	136	19	18	Positive
Oh-rosiglitazone	373.9>151.1	150	16	33	16	Positive
Oh-tolbutamide	284.9>189.6	150	-20	-42	-11	Positive
Oh-mephenytoin	235.1>150.2	150	56	27	10	Positive
Dextropan	258.1>157	150	191	53	12	Positive
β -estradiol-3-Glucuronide	447>271	200	-77	-52	-23	Negative
Trifluoperazine- N-Glucuronide	584>408	200	45	22	39	Positive
Serotonin-O-Glucuronide	353>160	200	34	33	3	Positive
Propofol-O-Glucuronide	353.1>177.1	200	-32	-34	-2	Negative
AZT-5'-Glucuronide	442>125	200	-55	-30	-1	Negative
Clorpropamide	277>175	150	120	20	12	Positive
Clorpropamide	274.9>189.6	150	-80	-50	-12	Negative
Theophylline	181.1>124.1	200	27	40	10	Positive
Theophylline	179.1>163.9	200	-59	-20	-1	Negative
20-ginsenoside Rg3	783.4>161.1	150	-5	-44	-9	Negative
20-ginsenoside Rh2	621.3>161.1	150	-20	-30	-17	Negative
Diosin	867.2>761.5	150	-8.7	-43.6	-16.5	Negative

DP: Declustering Potential; CE: Collision Energy; CXP: Collision Cell Exit Potential

Data analysis

For reversible inhibition and time-dependent inhibition screening, the activities in the presence of inhibitors were expressed as percentages of the corresponding control values using the substrates. The remaining activities at the tested highest concentration lesser than 80% were considered to be “positive” and then the 50% inhibitory concentration (IC_{50}) values were extrapolated by nonlinear least-squares regression analysis using WinNonlin (ver. 4.0; Pharsight, Mountain View, CA, USA). The kinetic parameters for inhibitory potential (K_i) were initially estimated by graphical methods such as Dixon plot and Lineweaver–Burk plot, but ultimately determined by nonlinear least-squares regression analysis from the best enzyme inhibition model using Enzyme kinetic software. The mode of inhibition was determined on the basis of the Akaike information criterion, as a measure of the goodness of fit. The inhibition modes tested included pure and partial competitive inhibition, noncompetitive inhibition, mixed-type inhibition, and uncompetitive inhibition.

Pharmacokinetic parameters were calculated by a non-compartmental analysis using WinNonlin Professional, version 2.1 (Pharsight, Mountain View, CA, USA): the total area under the plasma concentration–time curve from time zero to infinity or the last measured time (AUC_t), and terminal half-life. The peak plasma concentration (C_{max}) and time to reach C_{max} (T_{max}) were read directly from the experimental data. The results were analyzed using

Student's t-test, with p value < 0.05 considered to statistical significance. All data are expressed as means standard deviation (SD), except median (range) for Tmax. The drug - drug interaction magnitude is affected by both in vitro inhibition kinetic parameters (Ki) and in vivo concentration of inhibitors. If the maximum plasma concentration (C_{max}) were as the [I] in vitro - in vivo extrapolation equation: $AUC_i/AUC = 1 + [I]_{in\ vivo}/K_i$, the ratio of C_{max}/K_i could help us to extrapolate the drug-drug interaction related the UGT enzymes.

C. RESULTS

Competitive inhibition of xanthophylls and fermented Ginseng extract on cytochrome P450 activities

The inhibitory effects of astaxanthin, β -cryptoxanthin, canthaxanthin, lutein and zeaxanthin on the activities of nine major human isozymes (CYP1A2, CYP2A6, CYP2B6, CYP2C8, CYP2C19, CYP2D6, CYP2E1, and CYP3A4/5) were shown in Figure 3, respectively. The inhibitory effects of BST204 and four ginsenosides on the activities of nine CYP isozymes are shown in Figure 4. Their IC_{50} values are shown in Table 3. IC_{50} determination illustrates the overall CYP inhibitory effect as a function of the test inhibitor concentration. Samples containing only cocktail substrate set at the around K_m value were considered 100 % activity and all velocity measurement of inhibitor with different concentration was compared to a percent of control velocity with no inhibitor. The IC_{50} values for the positive controls used in the reversible inhibition studies were in good agreement with published values according to an acceptable degree of accuracy (Yuan et al., 2002, Kim et al., 2005, Han et al., 2011). The basic assay to assess the interaction potential of inhibition is IC_{50} determination and the extrapolated IC_{50} values almost were significantly higher than the solubility limit except BST204 slightly inhibited CYP2C8 with IC_{50} 17.4 $\mu\text{g}/\text{mL}$ in competitive inhibition. All tested compounds did not show significant inhibition.

Table 3. IC₅₀ of astaxanthin, β -cryptoxanthin, canthaxanthin, lutein, zeaxanthin and fermented Ginseng extract BST204, ginsenoside Rg3 R-form, Rg3 S-form, Rh2 R-form and Rh2 S-form (R-Rg3, S-Rg3, R-Rh2, S-Rh2) on 9 CYP isozyme activities in pooled human liver microsomes.

IC ₅₀ (μ M)	Astaxanthin	β -cryptoxanthin	Canthaxanthin	Lutein	Zeaxanthin
CYP1A2	>5	>5	>5	>5	>5
CYP 2A6	>5	>5	>5	>5	>5
CYP 2B6	>5	>5	>5	>5	>5
CYP 2C8	>5	13.8	>5	>5	>5
CYP 2C9	>5	>5	>5	>5	>5
CYP 2D6	16.2	>5	10.9	>5	>5
CYP 2E1	>5	>5	>5	>5	>5
CYP 3A	>5	>5	>5	>5	>5
IC ₅₀ (μ M)	BST204 (μ g/mL)	R-Rg3 (μ M)	S-Rg3 (μ M)	R-Rh2 (μ M)	S-Rh2 (μ M)
CYP1A2	>20	>20	>20	>20	>20
CYP 2A6	>20	>20	>20	>20	>20
CYP 2B6	>20	>20	>20	>20	>20
CYP 2C8	17.4	>20	>20	>20	>20
CYP 2C9	>20	>20	>20	>20	>20
CYP 2D6	>20	>20	>20	>20	>20
CYP 2E1	>20	>20	>20	>20	>20
CYP 3A	>20	>20	>20	>20	>20

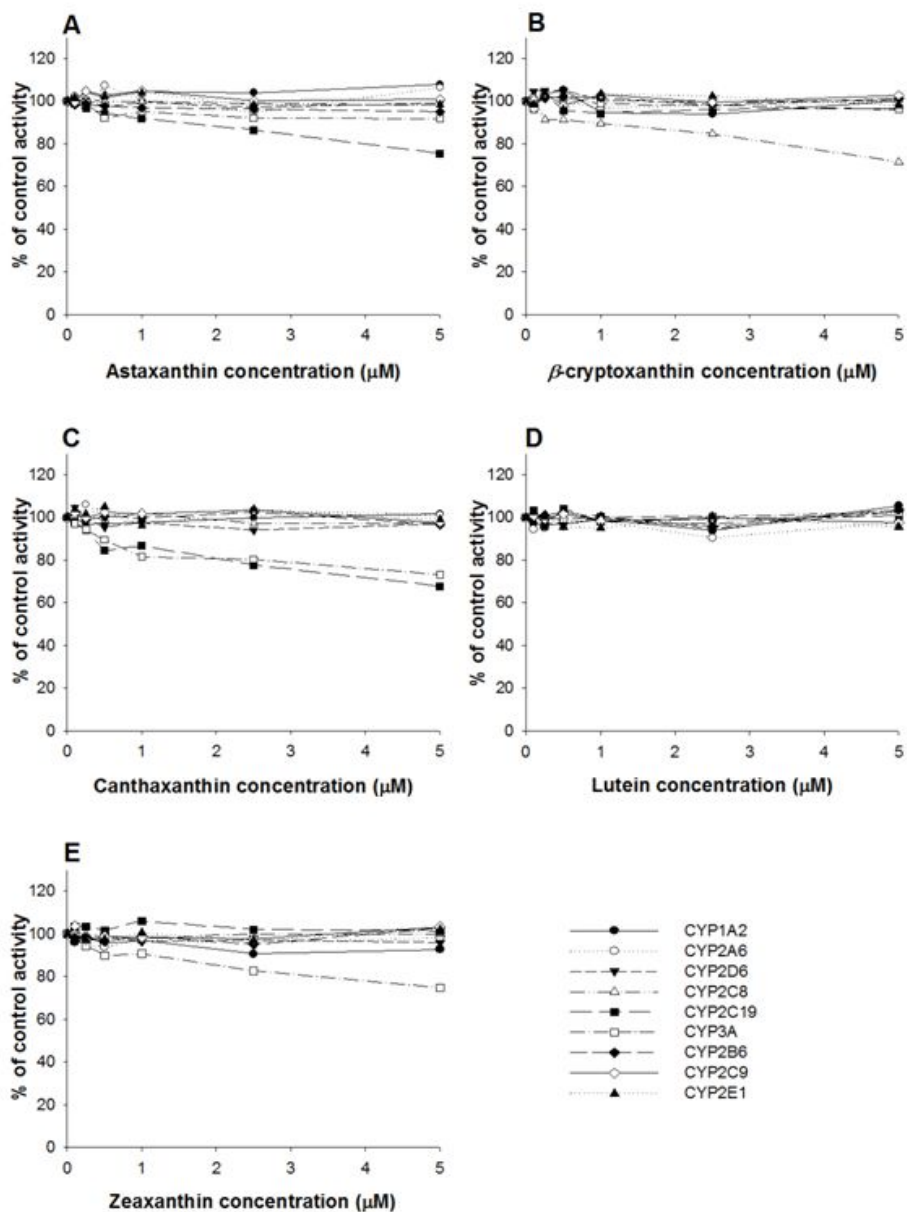


Figure 3. (A)~(E). Inhibition of CYP1A2, CYP2A6, CYP2B6, CYP2C8, CYP2C9, CYP2C19, CYP2D6, CYP2E1, and CYP3A4/5 by astraxanthin (A), β -cryptoxanthin (B), canthaxanthin (C), lutein (D), and zeaxanthin (E) in human liver microsomes. Each data point represents the mean value of triplicate determinations.

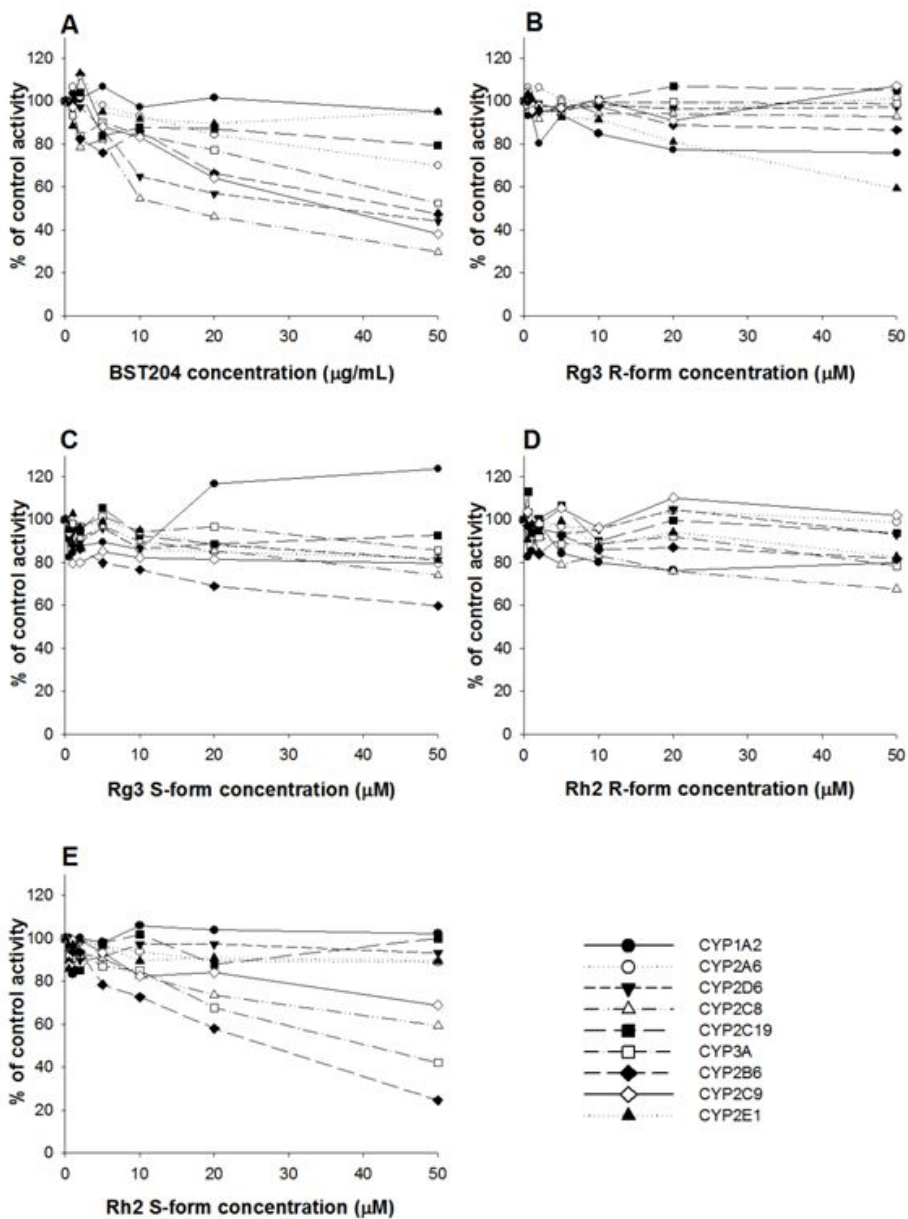


Figure 4. (A)~(E). Inhibitory effects of BST204, Rg3 R-form, Rg3 S-form, Rh2 R-form, and Rh2 S-form on 9 CYP isoforms in pooled human liver microsomes. The activity of each isoform was measured using respective specific probe substrate reaction. Represented by % of control activity.

Time-dependent inhibition of xanthophylls and fermented Ginseng extract on cytochrome P450 activities

Time-dependent inhibition is a term covering any phenomenon resulting in reduced enzyme activity with incubation time. Assessment of a change in the IC_{50} value with or without NADPH with the enzyme system is as straight forward and useful method for the initial determination of time-dependent inhibition effects (Obach et al. 2007; Fowler and Zhang, 2008). When the inhibition curve is shifted to a lower IC_{50} value by 30 min pre-incubation treatment, this is an indication of time-dependent inhibition. Upon 30 min pre-incubation of test compounds with human liver microsomes in the presence of NADPH, no obvious shift of IC_{50} was observed in the inhibition of the nine CYPs activities. Seen Figure 5, there was no IC_{50} shift for CYP3A4/5 by canthaxanthin with human liver microsomes. Time-dependent inhibitory effects of BST204 on nine CYP isozymes also suggested that the test compounds are not time-dependent inhibitors.

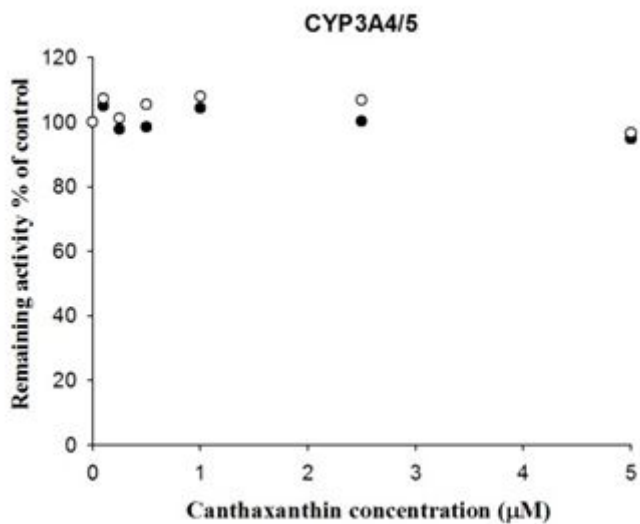


Figure 5. Representative IC_{50} shift plots for CYP3A4/5 by canthaxanthin with human liver microsomes in the presence (●) and absence (○) of NADPH for 30 min pre-incubation. Each data point represents the mean value of triplicate determinations. Vertical bars represent standard error of the mean.

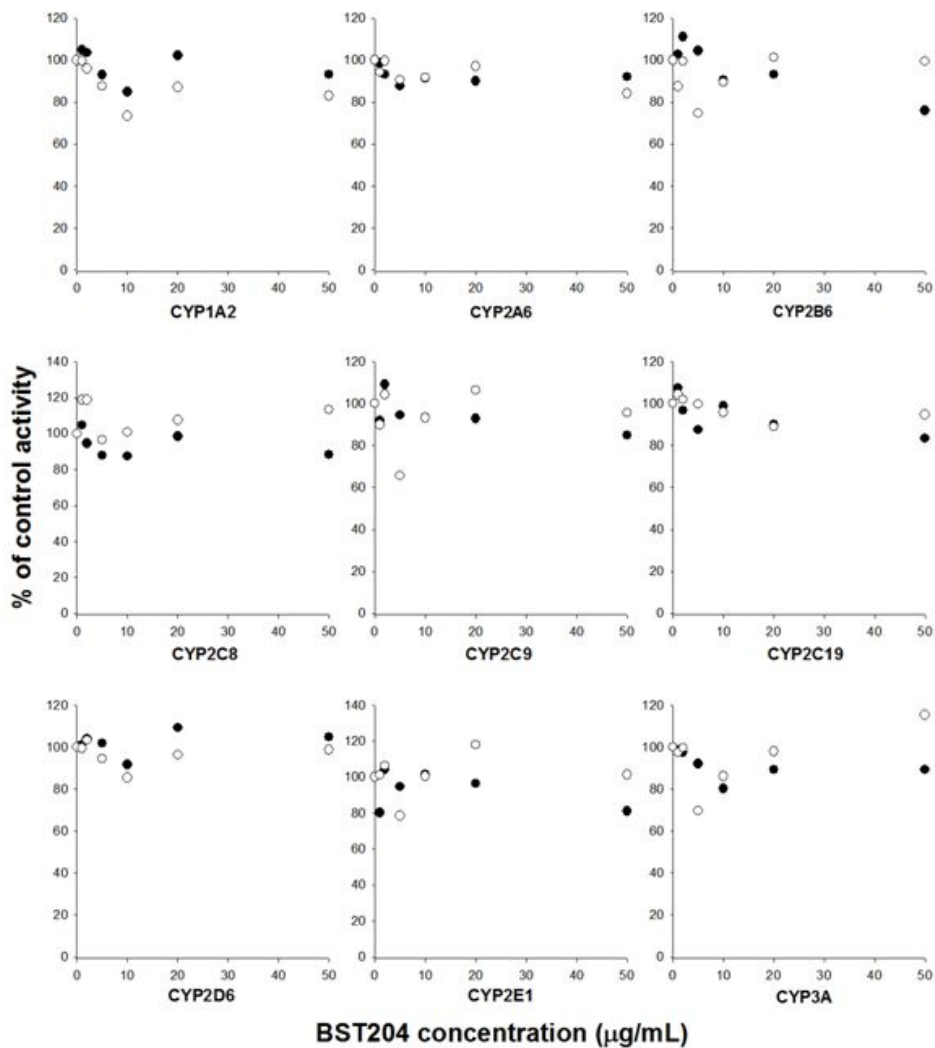


Figure 6. Time-dependent inhibitory effects of BST204 using IC_{50} shift assay on nine CYP isozymes. The activity of each isoform was measured using respective specific probe substrate reaction (●) with NADPH and (○) without NADPH). Represented by % of control activity. All experiments were conducted as duplicate.

Inhibitory effects of xanthophylls and fermented Ginseng extract on UGT isoform activities

As shown in Figure 7, the five xanthophylls were all demonstrated no inhibitory effect on UGT1A6, UGT1A9 and UGT2B7. But, β -cryptoxanthin, canthaxanthin and zeaxanthin showed inhibitory effects on UGT1A1 with IC_{50} values 23.68, 36.74 and 42.57 μ M, respectively, IC_{50} of β -cryptoxanthin and lutein on UGT1A4 were 28.66 and 29.94 μ M, respectively (Table 3). Astaxanthin did not show significant inhibition on the five kinds of UGT1A1 and UGT1A4. IC_{50} values of astaxanthin, β -cryptoxanthin, canthaxanthin, lutein and zeaxanthin on UGT1A1, UGT1A4, UGT1A6, UGT1A9, and UGT2B7 activities were evaluated and each substrate was listed in Table 3. The inhibitory effects of BST204, R-Rg3, S-Rg3, R-Rh2, and S-Rh2 on the activities of five UGT isozymes are shown in Table 4 and Figure 8. BST204 inhibited UGT1A1, 1A9, 2B7 with IC_{50} 13.80, 24.59, 30.83 μ g/mL, respectively. In addition, it was the S-form of Rg3, not R-form, that significantly inhibited UGT1A9, 2B7 with IC_{50} : 13.65, 21.95 μ M, respectively, IC_{50} of S-Rh2 on UGT1A1 was 77.75 μ M and the R-form of Rg3 and Rh2 showed ignorable inhibitory effects on UGT enzymes, we can deduce that it is the S-form of Rg3 and Rh2 that played an important inhibitory effects on UGT1A1, 1A9, 2B7 for BST204.

Table 4. IC₅₀ of astaxanthin, β -cryptoxanthin, canthaxanthin, lutein, zeaxanthin and fermented Ginseng extract BST204, ginsenoside Rg3 R-form, Rg3 S-form, Rh2 R-form and Rh2 S-form (R-Rg3, S-Rg3, R-Rh2, S-Rh2) on 5 UGT isozyme activities in pooled human liver microsomes.

IC ₅₀ (μ M)	Astaxanthin	β -cryptoxanthin	Canthaxanthin	Lutein	Zeaxanthin
UGT1A1	>50	23.68	36.74	>50	42.57
UGT1A4	>50	28.66	>50	24.94	>50
UGT1A6	>50	>50	>50	>50	>50
UGT1A9	>50	>50	>50	>50	>50
UGT2B7	>50	>50	>50	>50	>50
IC ₅₀	BST204 (μ g/mL)	R-Rg3 (μ M)	S-Rg3 (μ M)	R-Rh2 (μ M)	S-Rh2 (μ M)
UGT1A1	13.80	>100	>100	>100	77.75
UGT1A4	>100	>100	>100	>100	>100
UGT1A6	>100	>100	>100	>100	>100
UGT1A9	24.59	>100	13.65	>100	>100
UGT2B7	30.83	>100	21.99	>100	>100

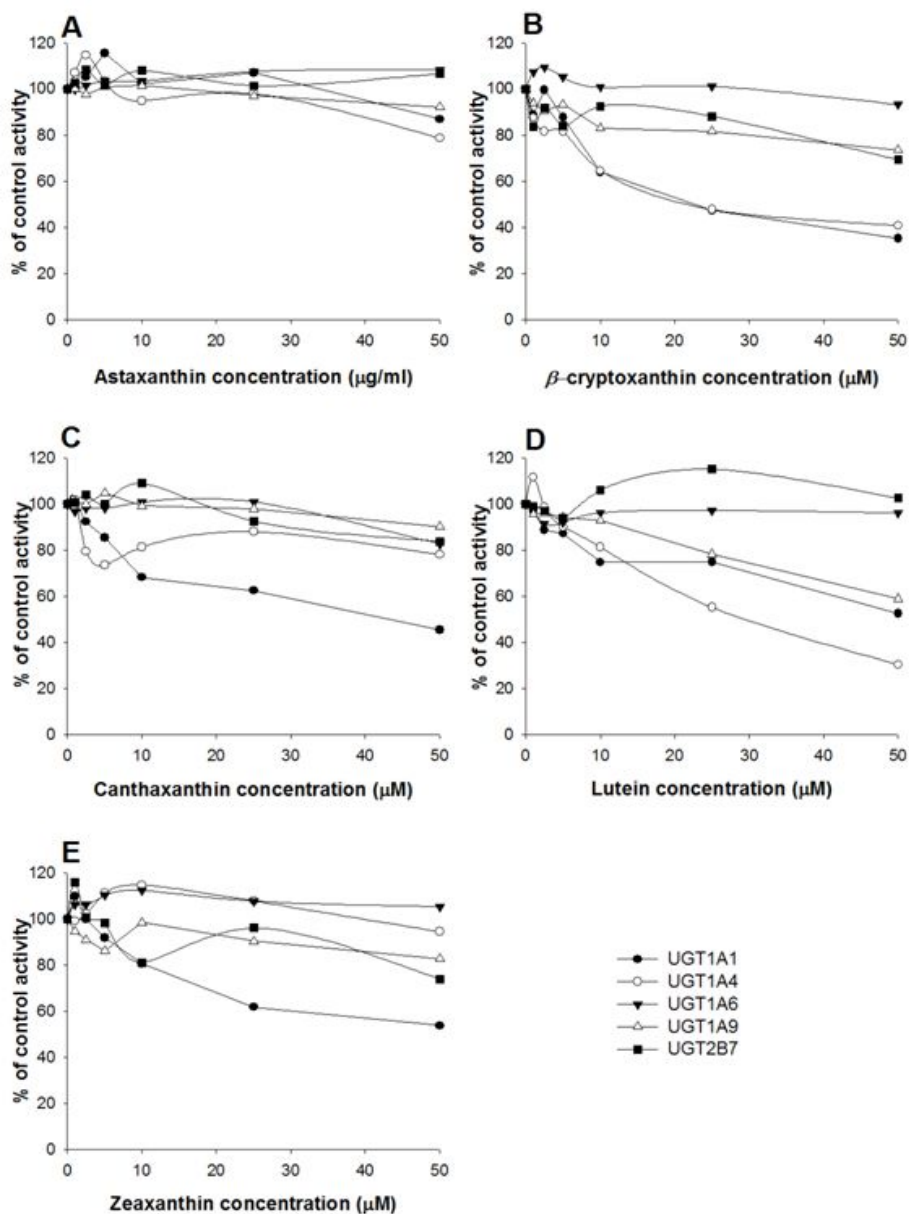


Figure 7. Inhibition of UGT1A1, UGT1A4, UGT1A6, UGT1A9 and UGT2B7 by astraxanthin(A), β -cryptoxanthin (B), canthaxanthin (C), lutein (D), and zeaxanthin (E) in human liver microsomes. Each data point represents the mean value of triplicate determinations.

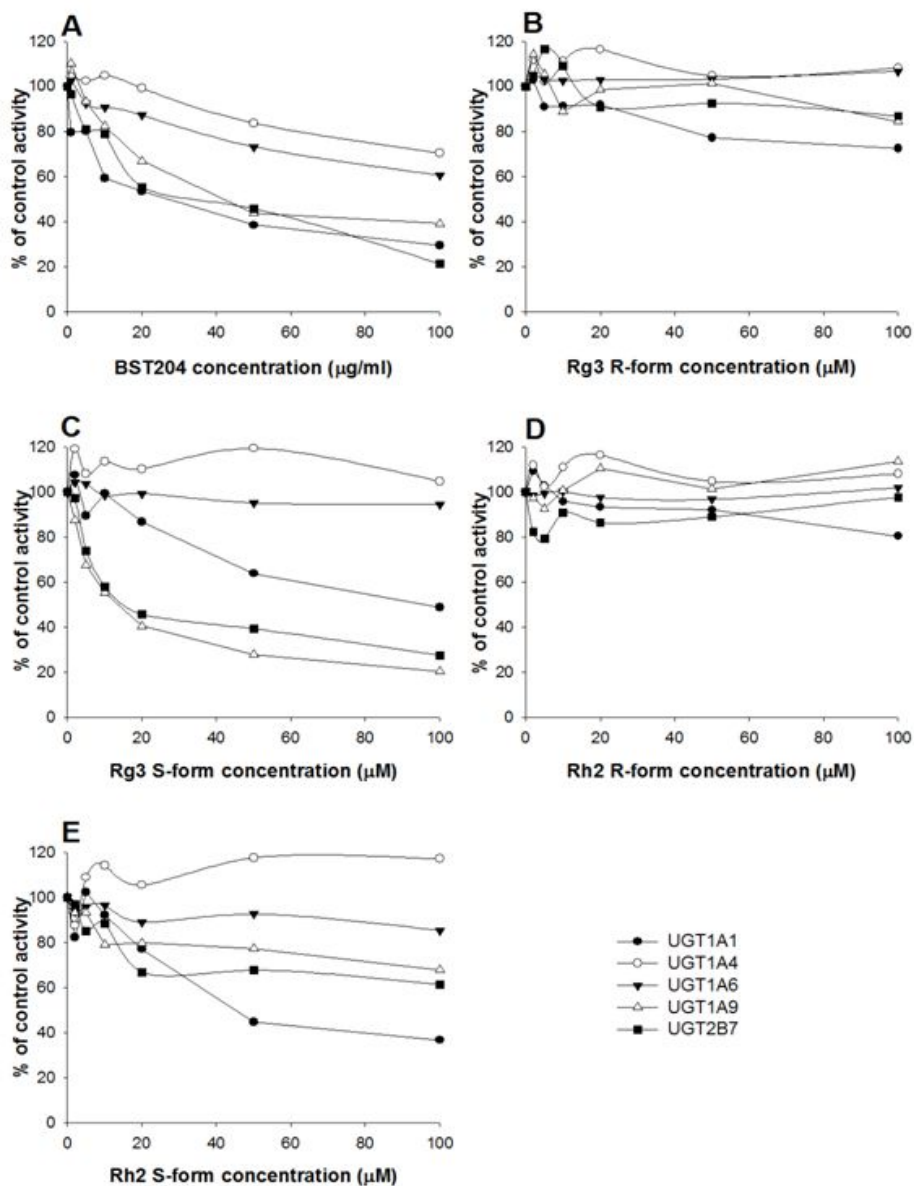


Figure 8. UGTs (UGT1A1, 1A4, 1A6, 1A9, 2B7) inhibitory effects of BST204, ginsenoside Rg3 R-form, Rg3 S-form, Rh2 R-form, and Rh2 S-form. The activity was measured using respective specific probe substrate reaction. Represented by % of control activity. All experiments were conducted as duplicate.

Ki determination of β -cryptoxanthin, BST204, S-Rg3 on UGT1A1, 1A9, 2B7

The Dixon plot and Lineweaver-Burk plot indicated that chrysin competitively inhibited the metabolism of estradiol in HLMS. The inhibition kinetic parameter (K_i) was calculated to be 306.51 μM . Like UGT1A1, niflumic acid, as the positive control, inhibited the metabolism of propofol in the competitive manner, which indicated by Dixon plot and Lineweaver-Burk plot and the inhibition kinetic parameter (K_i) was 0.1 μM . The K_i of efavirenz that competitively inhibited zidovudine metabolism was 50.79 μM .

As shown in Figure 9, the Dixon plot and Lineweaver-Burk plot indicated that β -cryptoxanthin competitively inhibited the metabolism of estradiol in HLMS. The inhibition kinetic parameter (K_i) was calculated to be 30.43 μM , which is much higher the C_{max} of β -cryptoxanthin in human plasma. As shown in Figure 11 and 12, kinetic parameters of BST204 on UGT1A1, 1A9, 2B7 enzymes were 27.38, 17.53, 32.51 $\mu\text{g/mL}$, respectively. The K_i of S-Rg3 inhibited UGT1A9 and 2B7 were 8.33 and 24.89 μM , respectively.

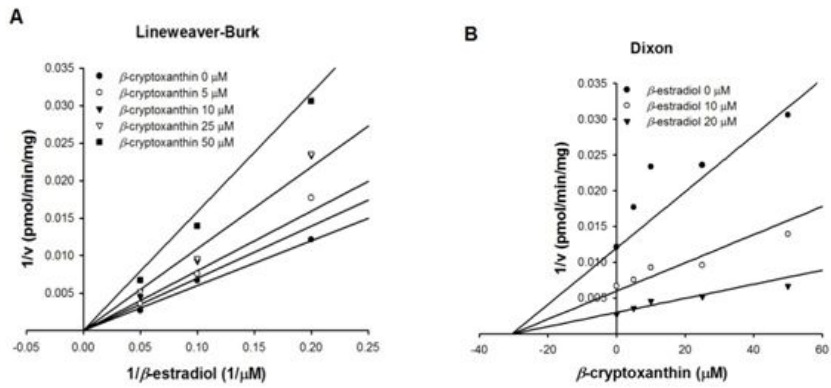


Figure 9. (A) Lineweaver–Burk plot and (B) Dixon plot about the K_i determination of β -cryptoxanthin towards UGT1A1-mediated glucuronidation. All the experiments were carried out in duplicate.

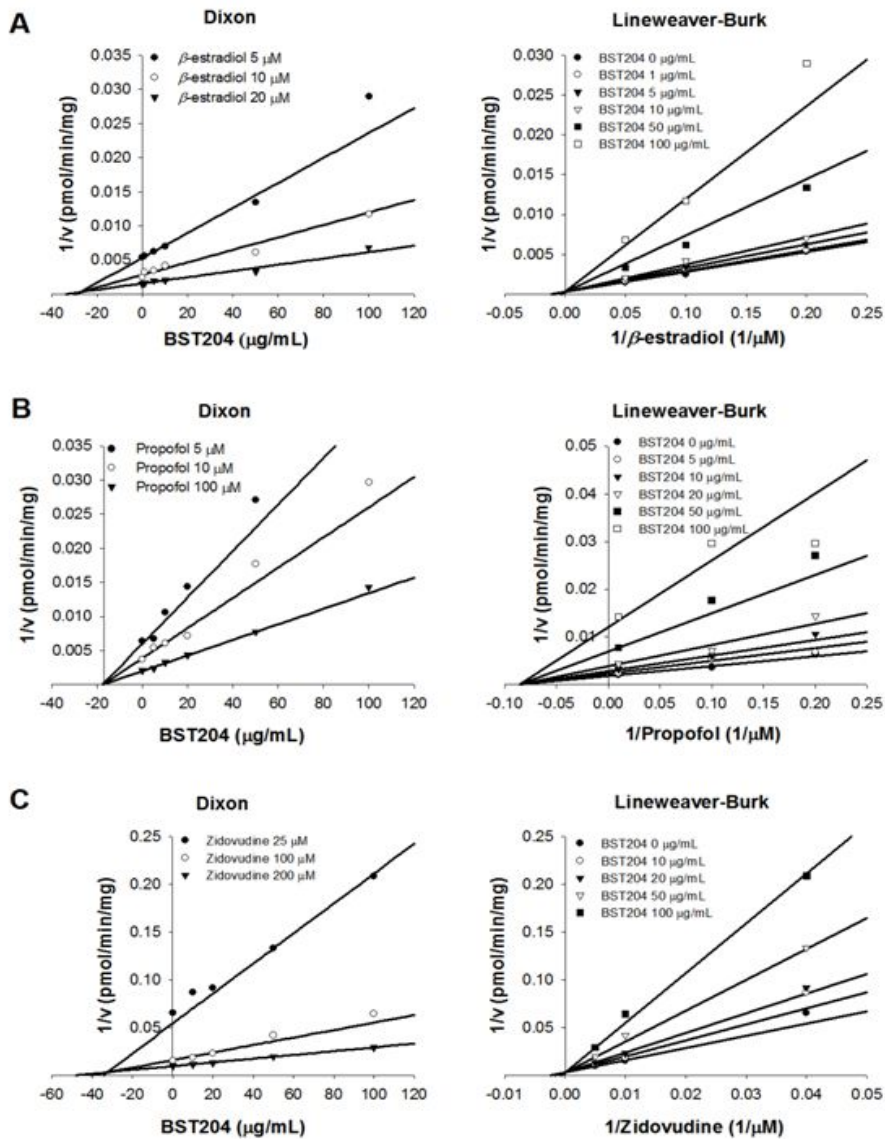


Figure 10. Dixon plot and Lineweaver-Burk plot about the K_i determination of BST204 towards UGT-mediated glucuronidation. (A) BST204 on UGT1A1-mediated estradiol glucuronidation; (B) BST204 on UGT1A9-mediated propofol glucuronidation; (C) BST204 on UGT2B7-mediated zidovudine glucuronidation. All the experiments were carried out in duplicate.

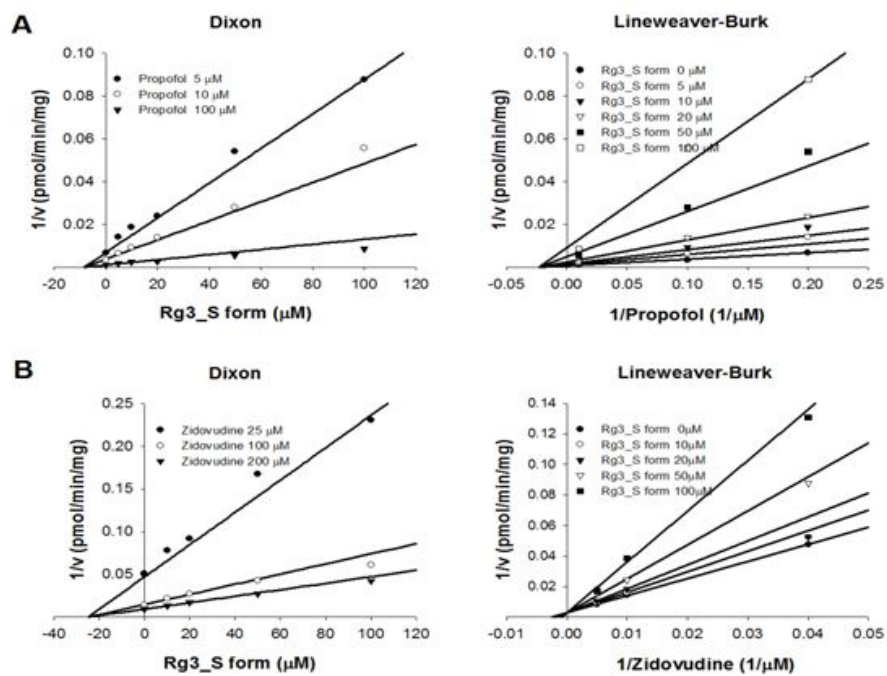


Figure 11. Dixon plot and Lineweaver-Burk plot about the K_i determination of ginsenoside Rg3 S-form towards UGT-mediated glucuronidation. (A) Ginsenoside Rg3 S-form on UGT1A9-mediated estradiol glucuronidation; (B) Ginsenoside Rg3 S-form on UGT2B7-mediated zidovudine glucuronidation. All the experiments were carried out in duplicate.

Pharmacokinetic studies of BST204 in human volunteers

For human pharmacokinetic parameters, the C_{max} of S-Rg3 and S-Rh2 were 4.84 and 102 ng/mL for 100 mg dosage, 6.93 and 273 ng/mL for 400mg dosage, respectively. The values of AUC_t of S-Rg3 were 1.61 and 3.38 $\mu\text{g min/mL}$ for the two doses, respectively. The most concentrations of S-Rh2 in 100 mg BST204 were below the detective limitation of our method, and the AUC_t of S-Rh2 was not calculated. Like rats pharmacokinetics, the R-form of Rg3 and Rh2 were also not found.

Table 5. Pharmacokinetic parameters of ginsenoside Rg3 S-form and Rh2 S-form (S-Rg3, S-Rh2) after single oral administration of BST204 extract at doses of 100 mg and 400 mg to healthy volunteer.

Parameters ^a	100 mg (<i>n</i> = 5)	400 mg (<i>n</i> = 5)
S-Rg3		
AUC _t (g min/mL) ^b	1.61 ± 0.81	3.38 ± 2.23
C _{max} (g/mL) ^c	0.00484 ± 0.00341	0.00693 ± 0.00283
T _{max} (min) ^d	240	240
S-Rh2		
AUC _t (g min/mL)	-	73.21 ± 25.89
C _{max} (g/mL)	0.102 ± 0.0582	0.275 ± 0.095
T _{max} (min)	120	120

a Values are mean ± standard deviation; b Total area under the plasma concentration –time curve from time zero to time last sampling time; c Peak plasma concentration; d Time to reach Cmax.Median(ranges).

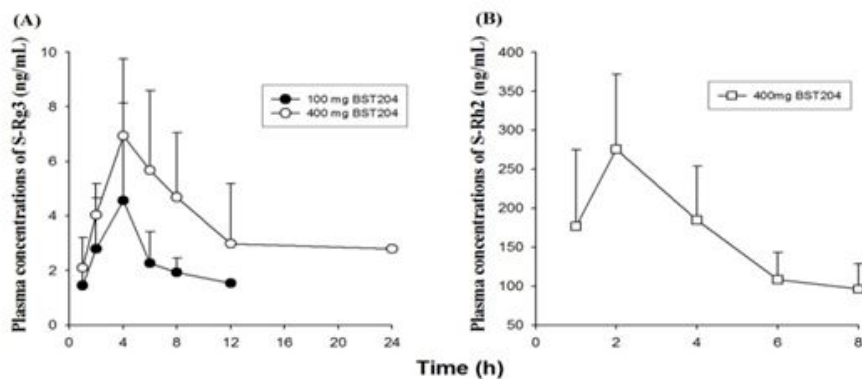


Figure 12. Mean plasma concentrations of ginsenoside Rg3 S-form (S-Rg3: A; circle) and ginsenoside Rg3 S-form (S-Rh2: B; square) after single oral administration of BST204 extract at doses of 100 mg (closed, n = 5) and 400 mg (open, n = 5) to human volunteers.

D. DISCUSSION & CONCLUSION

The concentration ranges used were based on solubility and the maximum plasma concentrations in vivo. Additionally, the organic solvents commonly used for assessment of in vitro activities with CYPs in human liver microsomes are methanol, acetonitrile, acetone, and dimethyl sulfoxide (DMSO). For lipophilic chemicals, using a percentage of organic solvent in any kinetic incubation, < 0.5% final (v/v) is recommended to sustain P450 activity. However, a higher content of DMSO is associated with stronger inhibition of CYP2C9, CYP2C19, CYP2D6, CYP2E1, and CYP3A activities in human liver microsomes (Chauret et al., 1998; Easterbrook et al., 2001). Additionally, a higher percentage of DMSO affects the sensitivity of MS/MS and is not recommended. Considering the poor solubility and DMSO limit, in our experiments, the tested xanthophylls were soluble in 0.5% DMSO (Lyan et al., 2001; Osterlie et al., 2000). The C_{max} values for astaxanthin, β -cryptoxanthin, canthaxanthin, lutein and zeaxanthin were 2.17, 0.15, 1.4, 1.05, and 0.15 μ M, respectively (Østerlie et al., 2000; Breithaupt et al., 2003; Paetau et al., 1997; Granado et al., 1998; Yu et al., 2012). The concentration ranges of the test compounds used covered them. Control samples (with no inhibitor) were assayed in each analytical run. The amount of metabolite in each sample (relative to control samples) was plotted versus the inhibitor concentration present to eliminate the impact of DMSO. BST204 and ginsenoside Rg3 and Rh2 were soluble in methanol and we studied the pharmacokinetics of BST204. Interestingly, Interestingly, we work found that the S epimers exhibited significantly higher concentrations and area under curve

values for both Rg3 and Rh2 in human plasma. The C_{max} of S-Rg3 in human plasma after administrated 100mg and 400 mg BST204 were 6.19 and 8.86 μM , respectively. Absorption and efflux mechanisms exhibited stereoselective regulations of P-gp (Yang et al., 2011). A study provides new evidence of the chiral characteristics of P-gp and is helpful to elucidate the stereoselective P-gp regulation mechanisms of ginsenoside Rh2 epimers in vivo from a pharmacokinetic view (Zhang et al., 2012). On the other hand, Rh2 is a good substrate of P-gp, and inhibition of P-gp can significantly enhance its oral bioavailability (Zhang et al., 2010).

The competitive inhibition results showed that the test compounds little inhibited the nine kinds of CYPs. Our results showed that the remaining activity percent of control were almost between 80-120% with each concentration ranges, on the other hand, the IC_{50} were much more than the highest concentrations of the designed concentration (except BST204 inhibited CYP2C8 with IC_{50} 17.4 $\mu\text{g}/\text{ml}$), no IC_{50} shifts illustrated that all the test compounds had no drug-interaction with CYPs in the long time and people can co-administrate it with other drugs (Obach RS, et al., 2007).

The main pathway of conjugative metabolism for a wide variety of compounds is glucuronidation by UGTs. Human UDP-glucuronosyltransferase (UGT) exists as a superfamily of 22 proteins, which are divided into 5 families and 6 subfamilies on the basis of sequence identity. Members of the UGT1A and 2B subfamilies play a key role in terminating the biological actions and enhancing the renal elimination of non-polar (lipophilic) drugs from

all therapeutic classes (Rowland et al., 2013). Glucuronidation elimination pathway in phase II metabolites plays more and more important role in recent years. Glucuronidation reactions catalyzed by UGT isoforms account for >35% of all phase II drug metabolism (Kiang et al., 2005). In addition, glucuronidation serves as an elimination pathway for numerous structurally diverse endogenous and exogenous compounds (Miners et al., 2010), such as bilirubin, bile acids, fatty acids, steroid hormones, thyroid hormones and fat soluble vitamins (Burchell et al., 1995; Radomska-Pandya et al., 1999; Tukey et al., 2000). So interaction with UGTs is also cannot be ignored. Fang's research indicated that the ginsenosides' inhibition towards UGT isoforms might be an important reason for ginseng-drug interaction. They found that Rg3 and Rh2 inhibited UGT1A1, 1A6, 1A7, 1A8, 1A9, 1A10, 2B7, 2B15 in different levels. Rg3 competitively inhibited UGT1A7, 2B7 and 2B15-catalyzed 4-MU glucuronidation reaction, and exerted noncompetitive inhibition towards UGT1A8-catalyzed 4-MU glucuronidation. The inhibition parameters (K_i values) were calculated to be 22.6, 7.9, 1.9, and 2.0 μM for UGT1A7, 1A8, 2B7 and 2B15 (Fang et al., 2013). Combined with our, we can find that it is the S-form of Rg3 and Rh2 that played an important inhibitory effects on UGT1A, 1A9, 2B7 for BST204. These results implied that the stereochemistry of ginsenosides may play an important role in selective UGTs inhibitory activity.

As we known, the drug - drug interaction magnitude is affected by both *in vitro* inhibition kinetic parameters (K_i) and *in vivo* concentration of inhibitors. If the maximum plasma concentration

(C_{\max}) were as the $[I]$ in vitro-in vivo extrapolation equation: $AUC_i/AUC=1+[I]_{\text{in vivo}}/K_i$, the ratio of C_{\max}/K_i could help us to extrapolate the drug-drug interaction related the UGT enzymes. A pharmacokinetic study reported that a single dose carotenoid supplement containing esterified 1.3 mg β -cryptoxanthin in healthy subjects, the mean C_{\max} was approximately 0.15 mM (Breithaupt et al., 2003), so the ratio of C_{\max}/K_i was much less than 0.1, which means there is very low risk of interaction. If the maximum plasma concentration (C_{\max}) of S-Rg3 was as the $[I]$ in vitro-in vivo extrapolation equation: $AUC_i/AUC=1 + [I]_{\text{in vivo}}/K_i$, the ratio of C_{\max}/K_i could help us to extrapolate that S-Rg3 and BST204 may interact with UGTs. But we cannot draw conclusion based on it and the reasons are as followings. More pharmacokinetic parameters of BST204 in human volunteers are insufficient, for example, the free concentration of Rg3 in human blood, the highest concentrations and the steady state concentration of Rg3 in human sample, so $[I]_{\text{in vivo}}/K_i$ may be different significantly; Thus, the in vivo interaction study is still needed.

Based on the IC_{50} values of these five xanthophylls on CYP and UGTs were marked greater than the C_{\max} values reported in human plasma, it is unlikely that these five xanthophylls, astaxanthin, β -cryptoxanthin, canthaxanthin, lutein, and zeaxanthin, from the diet or nutritional supplements alter the pharmacokinetics of drugs metabolized by CYPs or UGTs. On the other hand, further study about BST204, fermented ginseng extract, on the inhibition of UGT1A1, UGT1A9, UGT2B7 are still needed. These findings provide

some useful information for the safe and effective use of these herbs in clinical practice.

E. REFERENCES

- Attele AS, Wu JA, Yuan CS (1999) Ginseng pharmacology: multiple constituents and multiple actions. *Biochem Pharmacol* 58, 1685 - 1693.
- Bailey DG, Dresser GK (2004) Natural products and adverse drug interactions. *CMAJ* 170, 1531-1532.
- Bélanger AS, Caron P, Harvey M, Zimmerman PA, Mehlotra RK, Guillemette C (2009) Glucuronidation of the antiretroviral drug efavirenz by UGT2B7 and an in vitro investigation of drug-drug interaction with zidovudine. *Drug Metab Dispos* 37, 1793-1796.
- Bone RA, Landrum JT, Fernandez L, Tarsis SL (1988) Analysis of the macular pigment by HPLC: retinal distribution and age study. *Invest. Ophthalmol. Vis. Sci* 29, 843 - 849.
- Breithaupt DE, Weller P, Wolters M, Hahn A (2003) Plasma response to a single dose of dietary beta-cryptoxanthin esters from papaya (*Carica papaya* L.) or non-esterified beta-cryptoxanthin in adult human subjects: a comparative study. *Br J Nutr* 90(4), 795-801.
- Burchell B, Brierley CH, & Rance D (1995) Specificity of human UDP-glucuronosyltransferases and xenobiotic glucuronidation. *Life Sci* 57(20), 1819-1831.
- Chauret N, Gauthier A, Nicoll-Griffith DA (1998) Effect of common organic solvents on in vitro cytochrome P450-mediated metabolic activities in human liver microsomes. *Drug Metab Dispos* 26, 1-4.
- Chen CF, Chiou WF, Zhang JT (2008) Comparison of the pharmacological effects of *Panax ginseng* and *Panax quinquefolium*. *Acta Pharmacol Sin* 29, 1103 - 1108.
- Easterbrook J, Lu C, Sakai Y, Li AP (2001) Effects of organic

- solvents on the activities of cytochrome P450 isoforms, UDP-dependent glucuronyl transferase, and phenol sulfotransferase in human hepatocytes. *Drug Metab Dispos* 29, 141-144.
- Fang ZZ, Cao YF, Hu CM, Hong M, Sun XY, Ge GB, Liu Y, Zhang YY, Yang L, Sun HZ (2013) Structure-inhibition relationship of ginsenosides towards UDP-glucuronosyltransferases (UGTs). *Toxicol Appl Pharmacol* 267, 149-154.
- FDA, Center for Drug Evaluation and Research (CDER). (2012) Guidance for industry. Drug interaction studies-study design, data analysis, implication for dosing, and labeling recommendations. Draft guidance.
- Fujiwara R, Nakajima M, Yamanaka H, Katoh M, Yokoi T (2008) Product inhibition of UDP-glucuronosyltransferase (UGT) enzymes by UDP obfuscates the inhibitory effects of UGT substrates. *Drug Metab Dispos* 36, 361-367.
- Fowler S, Zhang H (2008) In vitro evaluation of reversible and irreversible cytochrome P450 inhibition: current status on methodologies and their utility for predicting drug-drug interactions. *AAPS J* 10, 410 - 424.
- Gradelet S, Astorg P, Leclerc J, Chevalier J, Vernevaut MF, Siess MH (1996) Effects of canthaxanthin, astaxanthin, lycopene and lutein on liver xenobiotic-metabolizing enzymes in the rat. *Xenobiotica* 26, 49-63.
- Granado F, Olmedilla B, Gil - Martínez E, Blanco I (1998) Lutein ester in serum after lutein supplement in human subjects. *Br. J. Nutr* 80, 445 - 449.

- Handelman GJ, Dratz EA, Reay CC, van Kuijk JG (1988) Carotenoids in the human macula and whole retina. *Invest. Ophthalmol. Vis. Sci* 29, 850 - 855.
- Higuera-Ciapara I, Felix-Valenzuela L, Goycoolea FM (2006) Astaxanthin: a review of its chemistry and applications. *Crit Rev Food Sci Nutr* 46, 185-196.
- Hussein G, Sankawa U, Goto H, Matsumoto K, Watanabe H (2006) Astaxanthin, a carotenoid with potential in human health and nutrition. *J Nat Prod* 69, 443-449.
- Jewell C, O'Brien NM (1999) Effect of dietary supplementation with carotenoids on xenobiotic metabolizing enzymes in the liver, lung, kidney and small intestine of the rat. *Br J Nutr* 81, 235-242.
- Kiang TK, Ensom MH, Chang TK (2005) UDP-glucuronosyltransferases and clinical drug-drug interactions. *Pharmacol Ther* 106(1), 97-132.
- Kim MJ, Kim H, Cha IJ, Park JS, Shon JH, Liu KH, Shin JG, (2005) High-throughput screening of inhibitory potential of nine cytochrome P450 enzymes in vitro using liquid chromatography/tandem mass spectrometry. *Rapid Commun. Mass Spectrom* 19, 2651 - 2658.
- Kistler A, Liechti H, Pichard L, Wolz E, Oesterhelt G, Hayes A, Maurel P (2002) Metabolism and CYP-inducer properties of astaxanthin in man and primary human hepatocytes. *Arch Toxicol* 75, 665-675.
- Krishnaswamy S, Duan SX, Von Moltke LL, Greenblatt DJ, Court MH (2003) Validation of serotonin (5-hydroxytryptamine) as an in

- vitro substrate probe for human UDP-glucuronosyltransferase (UGT) 1A6. *Drug Metab Dispos* 31(1), 133-139.
- Li L, Chen X, Zhou J, Zhong D (2012) In vitro studies on the oxidative metabolism of 20(s)-ginsenoside Rh2 in human, monkey, dog, rat, and mouse liver microsomes, and human liver s9. *Drug Metab Dispos* 40, 2041-2053.
- Liu J, Shimizu K, Yu H, Zhang C, Jin F, Kondo R (2010) Stereospecificity of hydroxyl group at C-20 in antiproliferative action of ginsenoside Rh2 on prostate cancer cells. *Fitoterapia* 81, 902-905.
- Lorenzo Y, Azqueta A, Luna L, Bonilla F, Domínguez G, Collins AR (2009) The carotenoid beta-cryptoxanthin stimulates the repair of DNA oxidation damage in addition to acting as an antioxidant in human cells. *Carcinogenesis* 2009, 30(2), 308-314.
- Lyan B, Azaïs-Braesco V, Cardinault N, Tyssandier V, Borel P, Alexandre-Gouabau MC, Grolier P (2001) Simple method for clinical determination of 13 carotenoids in human plasma using an isocratic high-performance liquid chromatographic method. *J Chromatogr B Biomed Sci Appl* 751, 297-303.
- Ma L, Dou HL, Wu YQ, Huang YM, Huang YB, Xu XR, Zou ZY, Lin XM (2012) Lutein and zeaxanthin intake and the risk of age-related macular degeneration: a systematic review and meta-analysis. *Br. J. Nutr* 107, 350 - 359.
- Miners JO, Bowalgaha K, Elliot DJ, Baranczewski P, Knights KM (2011) Characterization of niflumic acid as a selective inhibitor of human liver microsomal UDP-glucuronosyltransferase 1A9:

- application to the reaction phenotyping of acetaminophen glucuronidation. *Drug Metab Dispos* 39, 644-652.
- Miners JO, Mackenzie PI, Knights KM (2010) The prediction of drug-glucuronidation parameters in humans: UDP-glucuronosyltransferase enzyme-selective substrate and inhibitor probes for reaction phenotyping and in vitro-in vivo extrapolation of drug clearance and drug-drug interaction potential. *Drug Metab Rev* 42(1), 196-208.
- Obach RS, Walsky RL, Venkatakrishnan K (2007) Mechanism-based inactivation of human cytochrome P450 enzymes and the prediction of drug-drug interactions. *Drug Metab Dispos* 35(2), 246-55.
- Osterlie M, Bjerkeng B & Liaaen-Jensen S (2000) Plasma appearance and distribution of astaxanthin E/Z and R/S isomers in plasma lipoproteins of men after single dose administration of astaxanthin. *J Nutr Biochem* 11, 482-490.
- Paetau I, Chen H, Goh NM, White WS (1997) Interactions in the postprandial appearance of beta-carotene and canthaxanthin in plasma triacylglycerol-rich lipoproteins in humans. *Am. J. Clin. Nutr* 66, 1133 - 1143.
- Radomska-Pandya A, Czernik PJ, Little JM, Battaglia E, Mackenzie PI (1999) Structural and functional studies of UDP-glucuronosyltransferases. *Drug Metab Rev* 31(4), 817-899.
- Richer S, Stiles W, Statkute L, Pulido J, Frankowski J, Rudy D, Pei K, Tsipursky M, Nyland J (2004) Double masked, placebo-controlled, randomized trial of lutein and antioxidant supplementation in the intervention of atrophic age-related macular

- degeneration: the Veterans LAST study. (Lutein Antioxidant Supplementation Trial). *Optometry* 75, 216 - 230.
- Rowland A, Miners JO, Mackenzie PI (2013) The UDP-glucuronosyltransferases: their role in drug metabolism and detoxification. *Int J Biochem Cell Biol* 45(6), 1121-1132.
- Seo JY, Lee JH, Kim NW, Kim YJ, Chang SH, Ko NY, Her E, Yoo YH, Kim JW, Lee BY, Lee HY, Kim YM, Choi WS (2005a) Inhibitory effects of a fermented ginseng extract, BST204, on the expression of inducible nitric oxide synthase and nitric oxide production in lipopolysaccharide-activated murine macrophages. *J Pharm Pharmacol* 57, 911 - 918
- Seo JY, Lee JH, Kim NW, Her E, Chang SH, Ko NY, Yoo YH, Kim JW, Seo DW, Han JW, Kim YM, Choi WS (2005b) Effect of a fermented ginseng extract, BST204, on the expression of cyclooxygenase-2 in murine macrophages. *Int Immunopharmacol* 5, 929 - 936.
- Shin YM, Jung HJ, Choi WY, Lim CJ (2013) Antioxidative, anti-inflammatory, and matrix metalloproteinase inhibitory activities of 20(S)-ginsenoside Rg3 in cultured mammalian cell lines. *Mol Biol Rep* 40, 269-279.
- Sommerburg O, Keunen JE, Bird AC, van Kuijk FJ (1998) Fruits and vegetables that are sources for lutein and zeaxanthin: the macular pigment in human eyes. *Br J Ophthalmol* 82, 907-910.
- Tukey RH, Strassburg CP (2000) Human UDP-glucuronosyltransferases: metabolism, expression, and disease. *Annu Rev Pharmacol Toxicol* 40, 581-616.

- Uchaipichat V, Mackenzie PI, Elliot DJ, Miners JO (2006) Selectivity of substrate (trifluoperazine) and inhibitor (amitriptyline, androsterone, canrenoic acid, hecogenin, phenylbutazone, quinidine, quinine, and sulfinpyrazone) "probes" for human udp-glucuronosyltransferases. *Drug Metab Dispos* 34, 449-456.
- Walsky RL, Bauman JN, Bourcier K, Giddens G, Lapham K, Negahban A, Ryder TF, Obach RS, Hyland R, Goosen TC (2012) Optimized assays for human UDP-glucuronosyltransferase (UGT) activities: altered alamethicin concentration and utility to screen for UGT inhibitors. *Drug Metab Dispos* 40(5), 1051-1065.
- Wang H, Yu P, Gou H, Zhang J, Zhu M, Wang ZH, Tian JW, Jiang YT, Fu FH (2012) Cardioprotective Effects of 20(S)-Ginsenoside Rh2 against Doxorubicin-Induced Cardiotoxicity In Vitro and In Vivo. *EvidBasedComplementAlternatMed* 2012,506214.
- Wei X, Su F, Su X, Hu T, Hu S (2012a) Stereospecific antioxidant effects of ginsenoside Rg3 on oxidative stress induced by cyclophosphamide in mice. *Fitoterapia* 83, 636-642.
- Wei X, Chen J, Su F, Su X, Hu T, Hu S (2012b) Stereospecificity of ginsenoside Rg3 in promotion of the immune response to ovalbumin in mice. *Int Immunol* 24, 465-471.
- Yang H, Yoo G, Kim HS, Kim JY, Kim SO, Yoo YH, Sung SH (2012) Implication of the Stereoisomers of Ginsenoside Derivatives in the Antiproliferative Effect of HSC-T6 Cells. *J Agric Food Chem* 60, 11759 - 11764.
- Yang Z, Gao S, Wang J, Yin T, Teng Y, Wu B, You M, Jiang Z, Hu M (2011) Enhancement of oral bioavailability of 20(S)-ginsenoside

- Rh2 through improved understanding of its absorption and efflux mechanisms. *Drug Metab Dispos* 39, 1866-1872.
- Yu B, Wang J, Suter PM, Russell RM, Grusak MA, Wang Y, Wang Z, Yin S, Tang G (2012) Spirulina is an effective dietary source of zeaxanthin to humans. *Br. J. Nutr.* (in press).
- Yuan JP, Peng J, Yin K, Wang JH (2011) Potential health-promoting effects of astaxanthin: a high-value carotenoid mostly from microalgae. *Mol Nutr Food Res* 55, 150-165.
- Yuan R, Madani S, Wei XX, Reynolds K, Huang SM (2002) Evaluation of cytochrom P450 probe substrates commonly used by the pharmaceutical industry to study in vitro drug interactions. *Drug Metab Dispos* 30, 1311 - 1319.
- Zhang C, Yu H & Hou J (2011) Effects of 20 (S) -ginsenoside Rh2 and 20 (R) - ginsenoside Rh2 on proliferation and apoptosis of human lung adenocarcinoma A549 cells. *Zhongguo Zhong Yao Za Zhi*, 36, 1670-1674.
- Zhang J, Zhou F, Niu F, Lu M, Wu X, Sun J, Wang G (2012) Stereoselective regulations of P-glycoprotein by ginsenoside Rh2 epimers and the potential mechanisms from the view of pharmacokinetics. *PLoS One* 7, e35768.
- Zhang J, Zhou F, Wu X, Gu Y, Ai H, Zheng Y, Li Y, Zhang X, Hao G, Sun J, Peng Y, Wang G (2010) 20(S)-ginsenoside Rh2 noncompetitively inhibits P-glycoprotein in vitro and in vivo: a case for herb-drug interactions. *Drug Metab Dispos* 38, 2179-2187.
- Zhao L, Sweet BV (2008) Lutein and zeaxanthin for macular degeneration. *Am. J. Health. Syst. Pharm* 65, 1232 - 1238.

F. ABSTRACT IN KOREAN

사람 간효소인 cytochrome P450와 UDP-glucuronyltransferases에 대한 억제효과에 초점을 맞춘 xanthophyll과 발효 인삼 추출물의 허브-약물 상호작용의 평가연구

허브 보충제와 건강보조식품의 폭넓은 관심으로 인해 허브-약물간의 상호작용에 대해서도 최근에 많은 주목을 받아오고 있다. 주요 xanthophyll인 astraxanthin, β -cryptoxanthin, canthaxanthin, lutein, zeaxanthin은 항산화 효과를 가지거나 암 또는 노인성 황반변성을 예방하는 역할로 널리 사용되고 연구되어 왔다. BST204는 Rh2와 Rg3를 높은 농도로 함유하고 있던 새로 발효 인삼 추출물이다. Rh2와 Rg3는 가공하지 않은 인삼에서 ginsenoside- β -glucosidase에 의해 형성되며 산 조건하에서 가수분해를 통해 20(R)/20(S) ginsenoside Rg3 와 20(R)/20(S) ginsenoside Rh2이 더 풍부하게 만들어진다. 최근 연구에서 이 물질들이 항암효과를 보였다. 이 논문의 목적은 사람의 간 효소인 cytochrome P450와 UDP-glucuronyltransferase에 대한 다섯 종류의 xanthophyll (astraxanthin, β -cryptoxanthin, canthaxanthin, lutein, zeaxanthin)과 발효 인삼 추출물 BST204, 입체선택성 ginsenoside Rg3, Rh2 epimer의 9가지 CYPs, 5가지 UGTs에 대한 억제효과와 CYPs에 대한 유도효과에 상호작용을 평가하는 것이다.

USFDA 가이드라인에 따라 CYP1A2, CYP2A6, CYP2B6, CYP2C8, CYP2C9, CYP2C19, CYP2D6, CYP2E1 와 CYP3A에 대한 각각의 기질로써 phenacetin (50 μ M), coumarin (5 μ M), bupropion (50 μ M), rosiglitazone (1 μ M), tolbutamide (100 μ M), S-mephenytoin (100 μ M),

dextrophan (5 μ M), chlorzoxazone (50 μ M) 와 midazolam (5 μ M) 을 선택하였다. Competitive screening을 위해 실험물질인, cocktail, NADPH re-generating system, 사람 간 마이크로솜 (HLM)과 함께 5분 동안 pre-incubation 후에 15분간 incubation을 시행하였다. Time-dependent inhibition 실험도 진행하였다. Test compounds과 HLM을 NADPH 유무에 따라 37°C에서 30분간 incubation 하였고 이 후 기질 용액에 조금 옮겨 15분간 incubation 하였다. UGT1A1, UGT1A4, UGT1A6, UGT1A9 와 UGT2B7에 대한 각각의 기질로써 β -estradiol (10 μ M), trifluoperazine (40 μ M), serotonin (4000 μ M), propofol (100 μ M) 와 zidovudine (100 μ M) 을 선택하였다. 실험물질과 HLM, Tris-HCl buffer (pH 7.5), $MgCl_2$ (5 mM), substrate, and alamethicin (25 μ g/mL)을 30분간 pre-incubation 한 후에 UDPCA를 첨가하여 37°C에서 30분 또는 60분간 incubation을 시행하였다.

실험 결과 xanthophyll과 발효 인삼 추출물은 9가지 CYP의 가역적, 비가역적 억제에 대해 무시할만한 효과를 보였다. 하지만 β -cryptoxanthin, canthaxanthin, zeaxanthin은 UGT1A1에 대해 각각 IC_{50} 23.68, 36.74, 42.57 μ M로 억제효과를 보였다. β -cryptoxanthin, lutein 역시 UGT1A4에 대해 억제효과를 보였다. UGT1A1에 대한 β -cryptoxanthin의 K_i 는 30.43으로 β -cryptoxanthin의 C_{max} 보다 훨씬 높았다. 따라서 5가지 xanthophyll은 시험관내에서 UGT에 대해 억제효과를 보이지 않음을 추측할 수 있었다. CYP와 UGT에 대한 5가지 xanthophyll의 IC_{50} 값은 이미 알려진 혈장농도에서의 C_{max} 값보다 현저하게 큰 값이었다. BST204는 각각 IC_{50} 값 13.80, 24.59, 30.83 μ M 으로 UGT1A1, 1A9, 2B7을 억제하였다. S-Rg3는 UGT1A9과 2B7에 대해 억제효과를 보였다. UGT1A1, 1A9, 2B7효소에 대한 BST204의 K_i 는 각각 27.38, 17.53, 32.51 μ g/mL 였다. UGT1A9과 2B7에 대한 S-Rg3의 K_i 는

각각 8.33와 24.89 μM 였다.

건강보조식품에 포함된 5가지 xanthophylls가 CYP나 UGT에 의해 대사되는 약물의 약동학에 영향을 주지 않을 것으로 보인다. 하지만 발효인삼 추출물BST204은 UGT1A1, 1A9, 2B7대한 추가 실험이 필요하다.

주요어: 허브-약물 상호작용, xanthophylls, BST204, 인삼 추출물,
LC-MS/MS

학번: 2011-30824

G. CURRICULUM VITAE

First Name: Yufen
Last Name: Zheng
Address: Building17, College of Medicine Seoul National
Univ., Yeongeon-dong, Jongno-gu, Seoul, Korea
Telephone: +82-10-6808-8586
E-mail Address: cathy8521@hotmail.com
Birth Date: 1985-02-01
Nationality: China

Educational Background:

Mar 2011–Present: Ph.D. Candidate
Clinical Pharmacy
Department of Pharmacy
Graduate School
Seoul National University
Seoul, Korea

Sep 2007–Jun 2010: Master Degree
Clinical Pharmacy
Department of Pharmacy
Graduate School
China Pharmaceutical University
Nanjing, China

Sep 2003–Jun 2007: Bachelor Degree
Pharmacy
Department of Pharmacy
Yanbian University
Yanji, China

Research Career and Interests

1. Herb/Drug-drug interaction focused on 9 CYPs and 5 UGTs *in vitro*.
2. Pharmacokinetics of Ginseng extract, BST204 and the interaction study in vivo
3. Simultaneous quantification of analytes by liquid chromatography-tandem mass spectrometry.

Research articles

1. **Zheng YF**, Bae SH, Kwon MJ, Park JB, Choi HD, Shin WG, Bae SK. Inhibitory effects of astaxanthin, β -cryptoxanthin, canthaxanthin, lutein, and zeaxanthin on cytochrome P450 enzyme activities. *Food Chem Toxicol.* 2013; 59:78-85.
2. Bae SH, **Zheng YF**, Yoo YH, Kim JY, Kim SO, Jang MJ, Seo JH, Bae SK. Stereoselective determination of ginsenosides Rg3 and Rh2 epimers in rat plasma by LC-MS/MS: application to a pharmacokinetic study. *J Sep Sci.* 2013; 36(12):1904-1912.
3. Bae SH, Kwon MJ, Choi EJ, **Zheng YF**, Yoon KD, Liu KH, Bae SK. Potent inhibition of cytochrome P450 2B6 by sibutramine in human liver microsomes. *Chem Biol Interact.* 2013; 205(1):11-19.
4. Choi EJ, Bae SH, Park JB, Kwon MJ, Jang SM, **Zheng YF**, Lee YS, Lee SJ, Bae SK. Simultaneous quantification of caffeine and its three primary metabolites in rat plasma by liquid chromatography-tandem mass spectrometry. *Food Chem.*

2013;141(3):2735-2742.

5. Lim SW, Doh KC, Jin L, Piao SG, Heo SB, **Zheng YF**, Bae SK, Chung BH, Yang CW. Oral administration of ginseng ameliorates cyclosporine-induced pancreatic injury in an experimental mouse model. PLoS One. 2013; 29:8(8).
6. Doh KC, Lim SW, Piao SG, Jin L, Heo SB, **Zheng YF**, Bae SK, Hwang GH, Min KI, Chung BH, Yang CW. Ginseng treatment attenuates chronic cyclosporine nephropathy via reducing oxidative stress in an experimental mouse model. Am J Nephrol. 2013; 37(5):421-433.
7. Soo Hyeon Bae, **Yu Fen Zheng**, Min Jo Kwon, Eu Jin Choi, Soo Kyung Bae. Establishment and Significance of Bioequivalence Recommendations for Individual Products-Drugs Acting on Circulatory System and Others. J Korean Soc Clin Pharmacol Ther. 2013; 21(1):17-25.

Poster Presentation:

1. **Yu Fen Zheng**, Soo Hyeon Bae, Min Jo Kwon, Jung Bae Park, Wan Gyoon Shin, Soo Kyung Bae. Food, supplements-drug interaction on nine cytochrome P450 enzyme activities with astaxanthin, β -cryptoxanthin canthaxanthin, lutein and zeaxanthin. 2012/07, Asian Conference on clinical pharmacy.
2. **Yufen Zheng**, Wangyoon Shin, Sookyung Bae. Inhibitory effects of astaxanthin, β -cryptoxanthin, canthaxanthin, lutein, and zeaxanthin on 5 UDP-glucuronosyltransferases (UGTs) enzyme

activities. 2013/12/09, American Society of Health-System Pharmacists (ASHP).